To the Graduate Council:

I am submitting herewith a thesis written by James Philip Rogers entitled "Introducing water vapor into a high vacuum chamber at AEDC." I have examined the final electronic copy of this thesis for form and content and recommend that it be accepted in partial fulfillment of the requirements for the degree of Master of Science, with a major in Aerospace Engineering.

Trevor M. Moeller, Major Professor

We have read this thesis
and recommend its acceptance:

Frank G. Collins

L. Montgomery Smith

Acceptance for the Council

Carolyn R. Hodges

Vice Provost and Dean of the Graduate School

INTRODUCING WATER VAPOR INTO A HIGH VACUUM CHAMBER AT AEDC

A Thesis

Presented for the

Master of Science

Degree

The University of Tennessee, Knoxville

James Philip Rogers

December, 2011

Dedication

This thesis is dedicated to my family. Thank you for all your love and support.

Acknowledgments

The Author wishes to express his deepest gratitude to everyone involved in helping him with this thesis. Thanks to my school for giving me the opportunity to continue my education. Thanks to my advisor, Dr. Trevor Moeller, for giving me such an interesting and involved project to work on, and for all his help, encouragement and patience throughout the process. Thanks to the rest of my Committee, Dr. Frank Collins and Dr. Monty Smith, for their help and technical expertise, which I could not have done without. Thanks to Jesse Labello and William Ring, who have also worked very hard with me on this project. Thanks to Doug Warnberg for helping me find all the equipment I needed and then helping me figure out how to put it all together. Thanks to Alexander Terekhov, Dr. Lino Costa, Dr. Abhilasha Verma, Dr. George Murray and Dr. Bill Hofmeister for for their willingness to help and for letting me use their equipment. Thanks to my family and all my friends for all of their encouragemnet and support. Thanks to the people at AEDC who supported this work. This work was supported by AEDC under contract number FA9101-06D-0001/0006.

Abstract

A powdered form of calcium sulfate dihydrate ($CaSO_4 \cdot 2H_2O$) was heated to provide water vapor in a vacuum chamber for an experiment seeking to study cryodeposit thin films of ice at the Arnold Engineering Development Center (AEDC) in Tullahoma, TN. However, after the test was conducted, calcium sulfate deposits were found on all surfaces inside the vacuum chamber. It became clear that a new procedure for introducing the water vapor into the vacuum chamber needed to be developed. Calcium sulfate dihydrate, cobalt(II) chloride hexahydrate and 3 angstrom zeolite molecular sieves were investigated to determine how they could be used to deliver water vapor into a vacuum system. An inductive heater was used to heat the samples, a residual gas analyzer to see what gases they released, and a microbalance to measure the mass of the samples as they were being tested inside the vacuum chamber. The 3 angstrom molecular sieves proved to be the most suitable material for these purposes, and a new method that uses them to deliver water vapor to a vacuum system was developed and has been tested in a vacuum chamber at the University of Tennessee Space Institute's (UTSI) Center for Laser Applications (CLA). This method, with the water source located in an external canister that allows the source to be replaced without breaking the vacuum of the vacuum chamber, has been successfully implemented at AEDC.

Contents

List of Tables

List of Figures

Chapter 1

Introduction

1.1 Overview and Purpose of this Thesis

Usually, researchers do everything in their power to keep water out of their vacuum systems, but the goal of this thesis has been to do just the opposite, to find a way to introduce water into the vacuum. When water molecules enter a cold vacuum chamber, they tend to condense and form icy deposits on any surface they contact. This becomes a problem when the ice starts to form on delicate and sensitive instruments. The ice can keep these instruments from working properly, prevent them from making accurate measurements, and sometimes it can cause them to fail completely. Ongoing research at the Arnold Engineering and Development Center (AEDC) and the University of Tennessee Space Institute (UTSI) is directed toward developing techniques that can be used to detect and mitigate the effects of cryodeposition inside vacuum systems. Part of that research involves developing an experimental procedure for growing thin films of ice on optical components inside a low-temperature, high-vacuum chamber. The ultimate goal of those experiments is to test, evaluate and develop new methods for detecting and mitigating the effects of cryodeposition inside vacuum chambers. To conduct these tests, a method is needed for introducing water vapor into the system in such a way that the water will condense and form thin layers of ice for testing.

Initial tests in the Ultra-High Vacuum Chamber (UHV) at AEDC used an effusion cell to create a free molecule plume of water vapor inside the vacuum chamber. The effusion

cell was made to contain and heat a small sample of calcium sulfate dihydrate powder which can hold up to two water molecules for each molecule of calcium sulfate. When heated, the calcium sulfate released its water molecules. This increased the pressure inside the effusion cell and pushed the free water molecules through a small hole at the front of the cell that was pointed toward cold test surfaces. The water molecules that escaped the effusion cell traveled to and condensed on the test surfaces and built up thin layers of ice.

Unfortunately, at the conclusion of the experiment, calcium sulfate was found throughout the vacuum chamber and on all the test surfaces inside the chamber. The experiment was designed to study thin layers of ice, and was not designed to tolerate any foreign contaminates other than water on the test surfaces. During the test, there was a problem with the effusion cell temperature control unit that might have overheated the calcium sulfate. Since it was such a fine powder, it was also possible that the calcium sulfate was carried out of the effusion cell by the flow of molecules leaving the cell. Regardless of what happened, new materials and new procedures for introducing the water needed to be investigated and developed to provide a more suitable way to introduce water vapor into the vacuum system.

1.2 Investigations Made in this Thesis

This thesis has been aimed to investigate the behavior of different materials and evaluate their ability to act as a suitable source of water inside a vacuum chamber. The outgassing dynamics of water vapor from calcium sulfate, cobalt chloride and 3Å molecular sieves have been studied at UTSI's Center for Laser Applications (CLA). These tests led to the development of a new method for introducing water vapor into a vacuum system.

To evaluate the usefulness of these materials, various tests were conducted to determine if and how these materials could be used to meet all the requirements of the cryodeposition tests: to provide pure water with even coverage on the test items. The cryotests were intended to study thin films of pure ice, so tests were conducted to see if and how water vapor could be extracted from these different materials. The goal of these tests was to determine how much water vapor a given material would provide and how easily it would provide it. These tests also sought to determine whether these materials would introduce any foreign contaminants other than water into the system or not. An inductive heater was used to heat the samples, a residual gas analyzer to see what gases were released, and a microbalance to measure the mass of the samples as they were being tested inside the vacuum chamber.

Once initial testing was complete, the molecular sieves were believed to be the most suitable choice for the cryo-tests, and the focus shifted from studying all three materials to developing a new test plan for using the zeolite. Further tests were run to study the outgassing dynamics of the sieves and to develop a technique to use them to provide the water vapor for the cryodeposition experiments. The technique that was eventually developed involves keeping the sieves in their own container that is connected to the main chamber by a valved feedthrough system. This method provides better control over the process by which the sieves start releasing water into the system, and allows samples to be changed in and out, mid-test, without having to open up the main chamber.

1.3 Background

The following sections provide some basic background information about the three materials studied in this thesis: calcium sulfate dihydrate, cobalt chloride hexahydrate and zeolite molecular sieves. These materials are commonly used as desiccants. Desiccants are hydroscopic substances that work though the absorption and/or the adsorption of water to induce or sustain a state of dryness in their local vicinity [6–8]. Adsorption occurs when a substance is chemically or physically bound to the surface of another material; absorption occurs when a substance is physically or chemically intergrated within another material, penetrating beyond its surface [9–12]. There are many different types of desiccants, and the way each type actually traps and takes in water can be different for each type. Most desiccants do not chemically combine with water or any of the other substances they are designed to capture. They instead capture them through weaker intermolecular forces (van der Waals forces, hydrogen bonding and other electrostatic interactions) between the moisture and surface of the desiccant [13].

Once these materials take in water, that water can be removed through a process called regeneration which separates the water moelcules from the desiccant. Typically, the regeneration process involves heating the desiccant in a vacuum chamber or some other water-free environment for some prescribed amount of time [7]. It is this regeneration process that was studied in this thesis in order to see how it could be used to provide water vapor for the cryodeposition tests. The following sections briefly describe what was known about each material and what material characteristics the experimental tests at UTSI needed to determine in order to evaluate how these materials could be used for the tests at AEDC.

1.3.1 Calcium sulfate dihydrate

Even though the calcium sulfate did not work well for the initial test, it was still studied with the hope that the problems that occurred during the first test could be avoided with a more careful approach or by making a few simple changes to the existing setup. Calcium sulfate occurs naturally in three forms: $CaSO_4$, called anhydrite, $CaSO_4 \cdot 0.5H_2O$, called hemihydrate or bassanite, and $CaSO_4{\cdot}2H_2O$, known as dihydrate or gypsum [14–16]. When

exposed to water, anhydrite readily transforms back into gypsum through adsorption, and instead of turning into a liquid or a paste like some materials, it will 'set' and maintain a relatively strong crystal lattice [15, 16].

Normally, gypsum must be heated to be dehydrated, and this process generally occurs in two steps [17]:

$$\text{(a) - } CaSO_4{\cdot}2H_2O + \text{heat} \rightarrow CaSO_4{\cdot}0.5H_2O + 1.5H_20$$
$$\text{(b) - } CaSO_4{\cdot}0.5H_2O + \text{heat} \rightarrow CaSO_4 + 0.5H_2O$$

In normal atmospheric conditions, the (a) reaction starts to occur at about 97°C [18], and the gypsum will start to transform into the calcium sulfate hemihydrate ($CaSO_4{\cdot}0.5H_20$). Temperatures as high as 163°C are required to start the (b) reaction and initiate the transition from bassanite to the water-free anhydrite [15]. However, these transition temperatures could be much lower in a vacuum chamber than they are for atmospheric conditions. Studies have shown that a decrease in relative humidity causes a decrease in the thermal stability of gypsum [19], and that the transition temperature for the gypsum to bassanite reaction monotonically shifts downward at lower pressures [18, 20].

Naturally occurring gypsum is 79% calcium sulfate and 21% water by weight [14]. A study has shown mass losses during the dehydration of gypsum at atmospheric pressures to be anywhere between 13.7% and 16.5% [21], and tests performed in a vacuum oven at the CLA gave similar results (14.9% - 15.4%) when a sample of calcium sulfate was heated at 100°C. For the initial test at AEDC, it was assumed that the calcium sulfate would not start releasing its water before being heated, but that needed to be confirmed. The exact temperature required to dehydrate the calcium sulfate in a vacuum was not known either, so that temperature needed to be found before the calcium sulfate could be used. Tests were needed to determine what temperature would initiate the release of water vapor and to see if there was a temperature that was high enough to vaporize the calcium sulfate or cause it to break down. Perhaps most importantly, a proceedure was needed that would keep the calcium sulfate inside the effusion cell and prevent if from blowing out into the vacuum chamber. If this could not be accomplished, then perhaps a non-powdered form of calcium sulfate could be found. Otherwise, the calcium sulfate probably would not be

the best candidate material for the cryodepostion tests.

1.3.2 Cobalt(II) chloride hexahydrate

Cobalt(II) chloride, $CoCl_2$, is another commonly used desiccant that is similar to calcium sulfate, but each molecule can hold six water molecules, whereas the calcium sulfate can only hold two. When it is dehydrated, $CoCl_2$ has a strong affinity for moisture and a very distinct blue color. When it is fully hydrated, via absorption, it forms a hexahydrate, $CoCl_2 \cdot 6H_20$, and has a deep purple color [1, 14, 22]. Like calcium sulfate, cobalt chloride can transition back and forth between its hydrated and dehydrated states with relative ease while still maintaining a strong solid crystalline structure. The color change and the easy transitions make it a useful indicator for water for many different applications. Photographs of anhydrous cobalt(II) chloride and the hexahydrate are given in Figure 1.1.

Figure 1.1: Anhydrous (left) and fully hydrated (right) cobalt(II) chloride [1].

The regeneration reactions involved in the equilibrium thermal decomposition of cobalt(II) chloride hexahydrate can be written as follows:

(a) - $CoCl_2 \cdot 6H_2O$ + heat $\rightarrow$ $CoCl_2 \cdot 4H_2O$ + $2H_2O$

(b) - $CoCl_2 \cdot 4H_2O$ + heat $\rightarrow$ $CoCl_2 \cdot 2H_2O$ + $2H_2O$

(c) - $CoCl_2 \cdot 2H_2O$ + heat $\rightarrow$ $CoCl_2 \cdot H_2O$ + H_2O

(d) - $CoCl_2 \cdot H_2O$ + heat $\rightarrow$ $CoCl_2$ + H_2O

In practice, the (a) and (b) reactions occur almost simultaneously and are virtually indistinguishable [2]. At atmospheric conditions, these reactions occur at 52-56°C and produce the violet-blue colored dihydrate form of cobalt(II) chloride. The (c) reaction starts at about 100°C to form a more violet colored monohydrate. The final (d) reaction starts around 120-140°C to produce the sky blue anhydrate [2]. A non-isothermal curve for these reactions, shown in Figure 1.2, is taken from a paper that describes the dehydration of cobalt chloride and shows that these reactions start at distinct temperatures at atmospheric pressures. Since this data is for atmospheric pressures, tests needed to be run to determine what the transition temperatures of cobalt chloride would be at vacuum conditions.

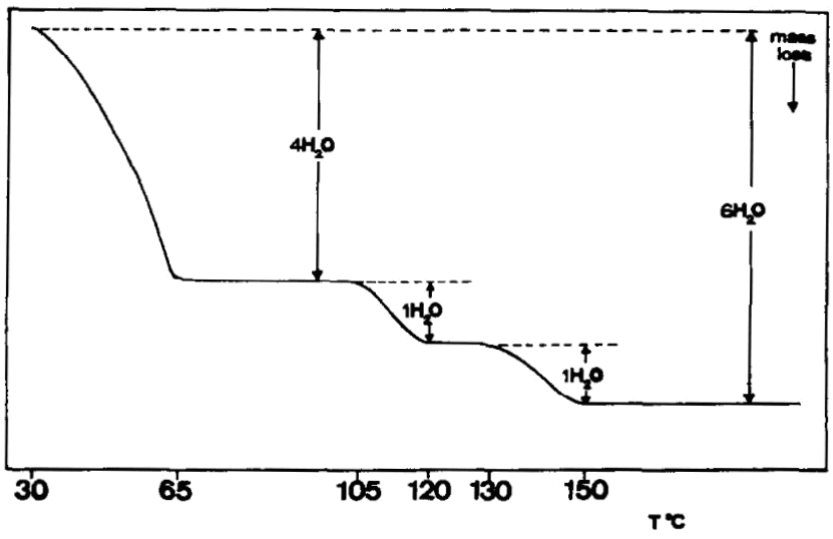

Figure 1.2: Dehydration reactions of cobalt(II) chloride [2].

The cobalt chloride was believed to work much the same way as the calcium sulfate would, but it might provide more water since it could hold six water molecules per molecule of solid material instead of just two. Fully hydrated cobalt chloride is 45% water and 55% solid material by weight [14]. It is also available in a more solid granular crystalline form, about the size of beach sand, which makes it a little more resistive to be being blown out of the effusion cell. However, MSDS forms indicate that cobalt chloride is a carcinogen and that there may be some serious health risks, such as cancer, associated with using it [23]. These health risks make the cobalt chloride a less attractive option even though it could potentially provide more water than the other two materials.

1.3.3 Zeolite molecular sieves

"Zeolite molecular sieves are crystalline, highly porous materials that are used for drying gases and liquids and for separating molecules on the basis of their size and shapes" [24]. They have an interconnecting network of crystalline micropores that form molecular sized voids and channels inside their crystalline structure. These channels form an internal surface area for the adsorption of molecules that are small enough to fit through the openings while excluding the molecules that are too large to fit in [24–29]. In addition, Zeolites also preferentially adsorb polar molecules [25] and have the ability to adsorb water from very dry enviroments [26, 29]. They are also known to release their water with the application of heat with almost no change to their crystalline structure [4, 29–31], which is how they got the name zeolite, which has Greek roots and means 'boiling stones'. The ability to 'sieve' molecules based on their size, shape or polarity is fairly unique to zeolites and makes them ideal for the adsorption of water from liquids or gases [4, 31].

Many types of zeolites can be used to adsorb different types of molecules, but this study is only interested in those that will adsorb water. Some of the most common types of zeolite used are the Linde A-type zeolites (LTA); designated by the size of the pore openings in their crystalline structure: 3Å, 4Å, 5Å, 8Å and 10Å. The 4Å type is known to adsorb H_2O, CO_2, SO_2, H_2S, C_2H_6, C_3H_6 and ethanol, while the 3Å type is said to only adsorb NH_3, H_2O and possibly some H_2 [4, 32]. Therefore, assuming that there would only be trace amounts of NH_3 and H_2 in the atmosphere, the 3Å type zeolite could be used to

adsorb water from the air without adsorbing other unwanted molecules.

To better understand how these molecular sieves work, it's helpful to take a closer look at a single LTA zeolite molecule (Figure 1.3). These zeolites are a class of alumniosilicate crystals made up of AlO_4 and SiO_4 molecules [26]. They form tetrahedras, and the "cages" that make up the basic building blocks for various types of zeolites. A single LTA molecule is composed of eight sodalite cages called β-cages that surround one central cage called the α-cage or the supercage (Figure 1.3). The β-cages have an average diameter of about 6.6Å, and each one can hold up to eight water molecules. The windows to these cages are 2.2Å wide, and most molecules are not small enough to fit inside them, but water molecules can still gain access through vibrational motion and dipole-cation interactions. Within the β-cages, water molecules will hydrogen-bond to each other or coordinate with oxygen atoms in the framework of the cell [3].

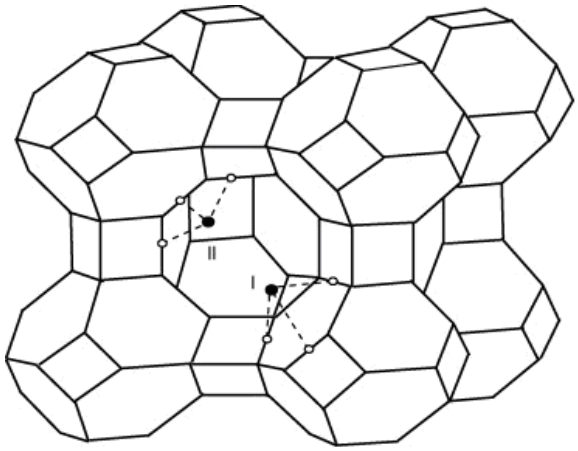

Figure 1.3: Framework of a unit cell of Linde type A zeolite. Eight sodalite cages (called β-cages) are cubically arranged around the central cavity (called the α-cage.) Cations are found at Sites I and II. Site I is located above the plane of a hexagonal face of a β-cage. Site II is located in the place of an octagonal window to the α-cage. [3].

The α-cage has a free diameter of about 11.4Å and can hold up to twelve water molecules [33]. Inside this cage, water molecules can hydrogen-bond with each other, coordinate with the oxygen atoms in the framework of the cell, and/or associate with cations that are also present in the cell. The water molecules enter the α-cage through windows that can be anywhere from 2.9Å to 4.8Å wide depending on the temperature of the molecule [4,29] and

on what cations are used during synthesis [34]. The presence of alumina in the framework gives the main structure of the zeolite an overall negative charge, which is counter-balanced by positive cations [26]. These ions actually project into the windows of the α-cage, and different ions can be used to fine tune the size of these openings. Using larger ions reduces the effective size of these windows, and using smaller ions make them bigger. 4Å zeolite is synthesized with sodium ions (r = 0.95Å) [34], but Linde 3Å zeolite is synthesized with larger potassium ions (r = 1.33Å) [35], which reduces the pore size from 4Å down to 3Å [3, 31] which is much closer to the size of a water molecule (2.7Å) [36]. The chart in Figure 1.4 shows the correlation between the effective pore size of various zeolites and the minimum kinetic diameters of the molecules that they can adsorb. Both the NaA type and KA type zeolite were studied in this thesis, but Figure 1.4 shows that the KA type (Linde 3Å) is probably the most suitable one for the purposes of this study, because it adsorbs fewer unwanted materials than any of the other types of zeolite.

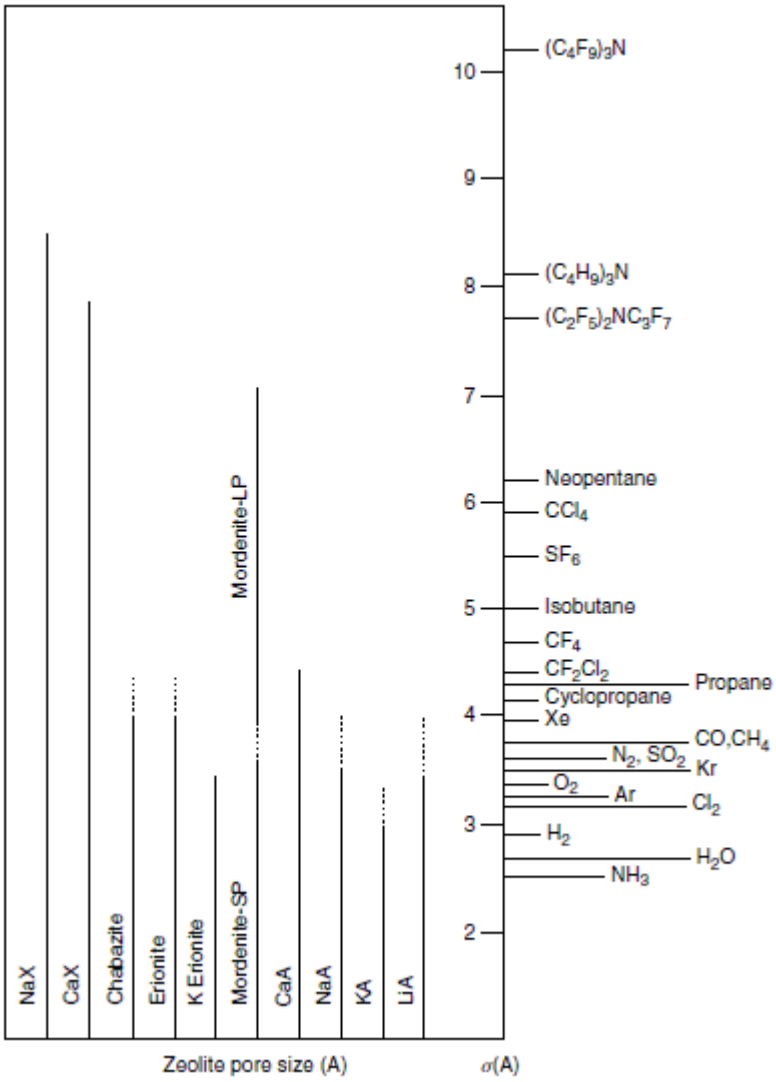

Figure 1.4: Correlation for molecular sieving molecules (with kinetic diameter σ) in various zeolites with different effective pore sizes at temperatures 77 K (solid lines) and 420 K (dotted lines) [4].

Figure 1.5 shows experimentally measured equilibrium adsorption isotherms for water vapor in zeolite 3Å first published by W. R.Grace and Co. [26] and redistributed by Mario Llano-Restrepo [3] to show the amount of water adsorbed [lbs of water per 100 pounds of zeolite 3Å] versus the ambient water vapor pressure [mm Hg or torr].

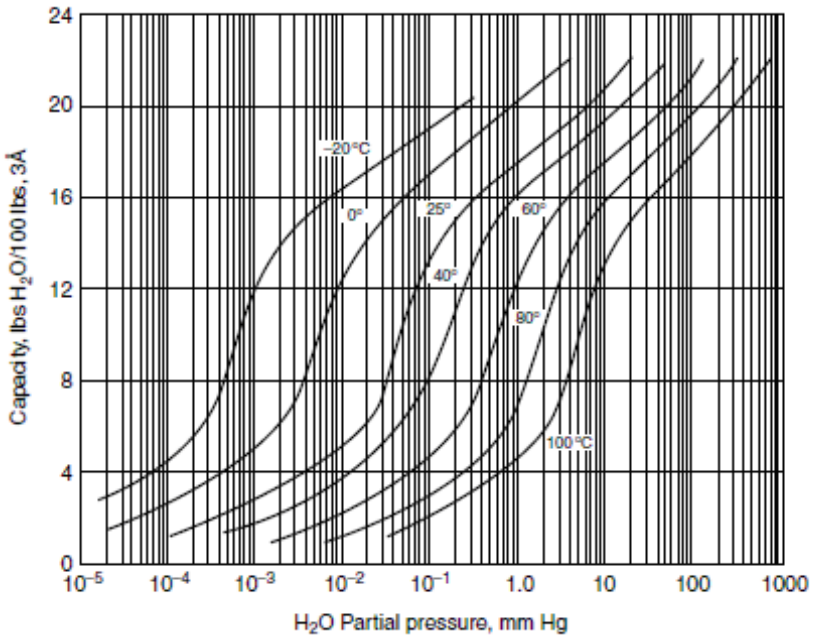

Figure 1.5: Equilibrium adsorption isotherms of water vapor in zeolite 3Å (KA type) at temperatures of: -20°C, 0°C, 25°C, 40°C, 60°C, 80°C, and 100°C [3].

These isotherms suggest that 3Å molecular sieves can be expected to hold an amount of water equal to about 20% of their empty mass. According to Breck [29], zeolites are dehydrated by heating them to a temperature of about 350°C in a vacuum of 10^{-5} torr, but these isotherms indicate that fully saturated molecular sieves should start to lose water as soon as the ambient water vapor pressure around them is decreased, even at low temperatures. So, unlike the calcium sulfate and the cobalt chloride, the molecular sieves should start releasing water in the vacuum chamber, even without adding any heat.

Therefore, a method that uses the molecular sieves to introduce water into the vacuum system would likely be very different than the one already developed for the calcium sulfate. In order to develop a new procedure, the outgassing dynamics of hydrated molecular sieves inside a vacuum chamber needed to be studied. Tests also needed to be run to ensure that

the zeolite does not introduce a significant amount of non-water contaminants and to see if the zeolite actually has the adsorptive capacity that was needed.

1.3.4 A proposed method for using zeolite molecular sieves

The proposed method for using the zeolite molecular sieves to provide the water vapor for the cryodeposit tests involves keeping the molecular sieves in their own separate container external to the main vacuum chamber. This container has a gas line with a valve on it that connects it to the main vacuum chamber. When the valve is closed, the main chamber can be pumped and cooled down, while the zeolite is kept at normal atmospheric conditions to keep it from unnecessarily losing its water. The external chamber also has another gas line that is connected to secondary vacuum pump that can be used to pump it down quickly before the valve to the main chamber test setup is opened. A schematic of this external chamber setup is given below in Figure 1.6, and a photograph is given in Figure 1.7. This configuration and its components are described in section 2.6.

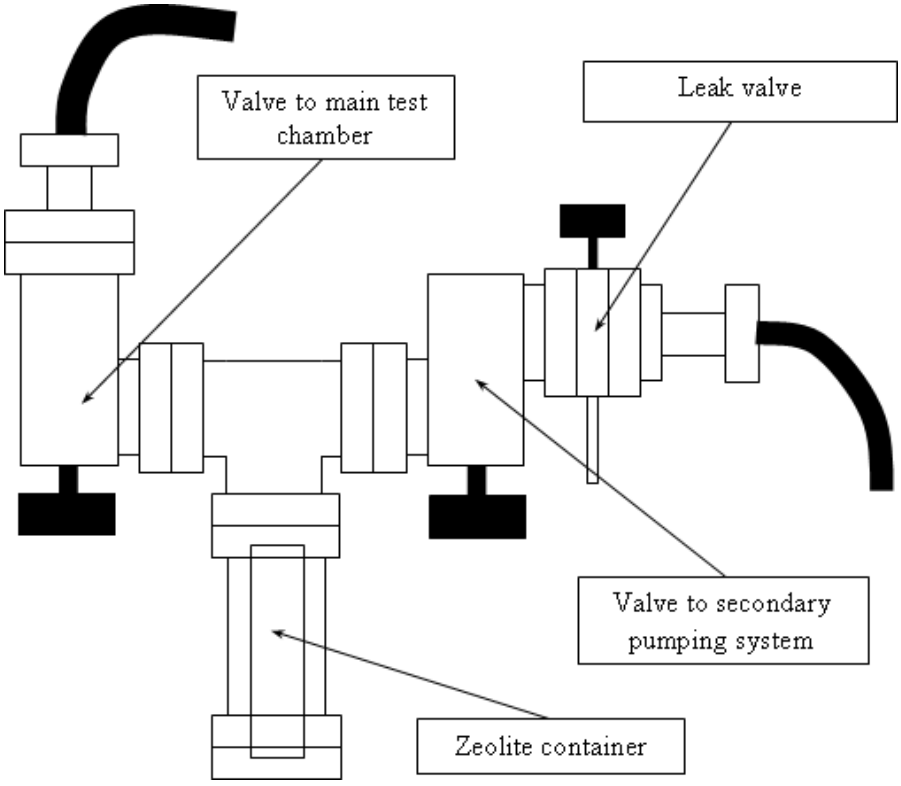

Figure 1.6: Schematic of the external chamber assembly.

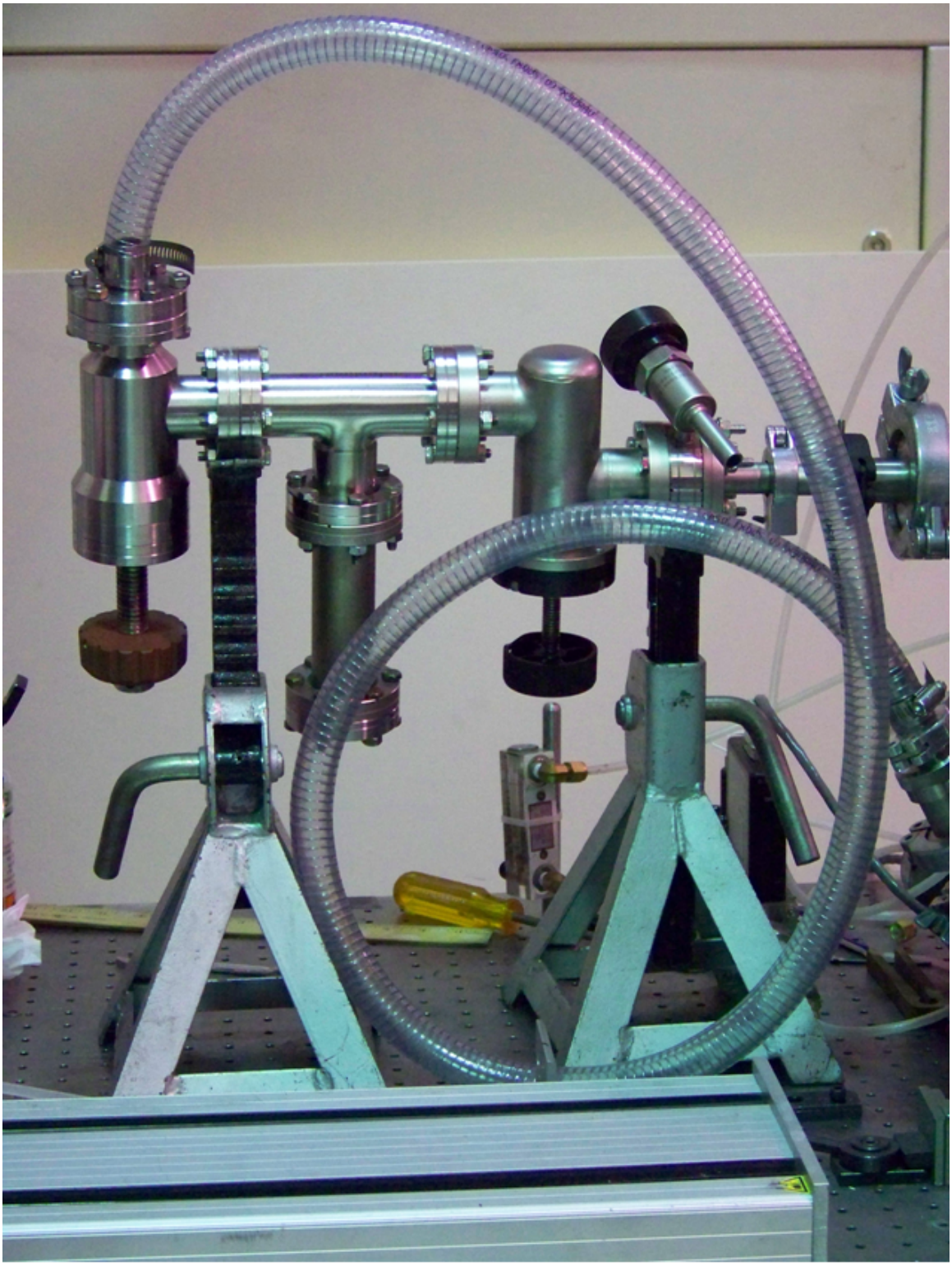

Figure 1.7: Photograph taken of the external chamber assembly.

Chapter 2

Test setups and instrumentation

The following sections briefly describe the various chamber configurations and the instruments used for each test.

2.1 Main chamber overview

A vacuum chamber at UTSI's Center for Laser Applications (CLA) was used to study and develop new methods for introducing water vapor into a vacuum system. The turbomolecular pumped chamber, shown in Figure 2.1, is capable of reaching pressures as low as 10^{-7} [torr], which is comparable to the base pressures obtained in the UHV chamber at AEDC. The chamber is equipped with a coiled inductive heater and a type T thermocouple that, together, were used to heat samples inside the vacuum chamber and measure their temperature. The vacuum chamber is also equipped with a residual gas analyzer (RGA), described in section 2.2. The RGA was used to characterize the gases inside the chamber and track their relative abundance. Internally, the chamber has an 11.5" x 11.0" base and is about 19" tall. This is large enough to hold an electronic A&D EJ120 compact balance (120 [g] capacity and a 0.01 [g] resolution) that was used to make time-resolved mass measurements of samples inside the vacuum chamber while it was in operation. These instruments, in various configurations, were used to help determine how stable each water source material is under vacuum, how much water they can provide, and at what rate that water is outgassed from them.

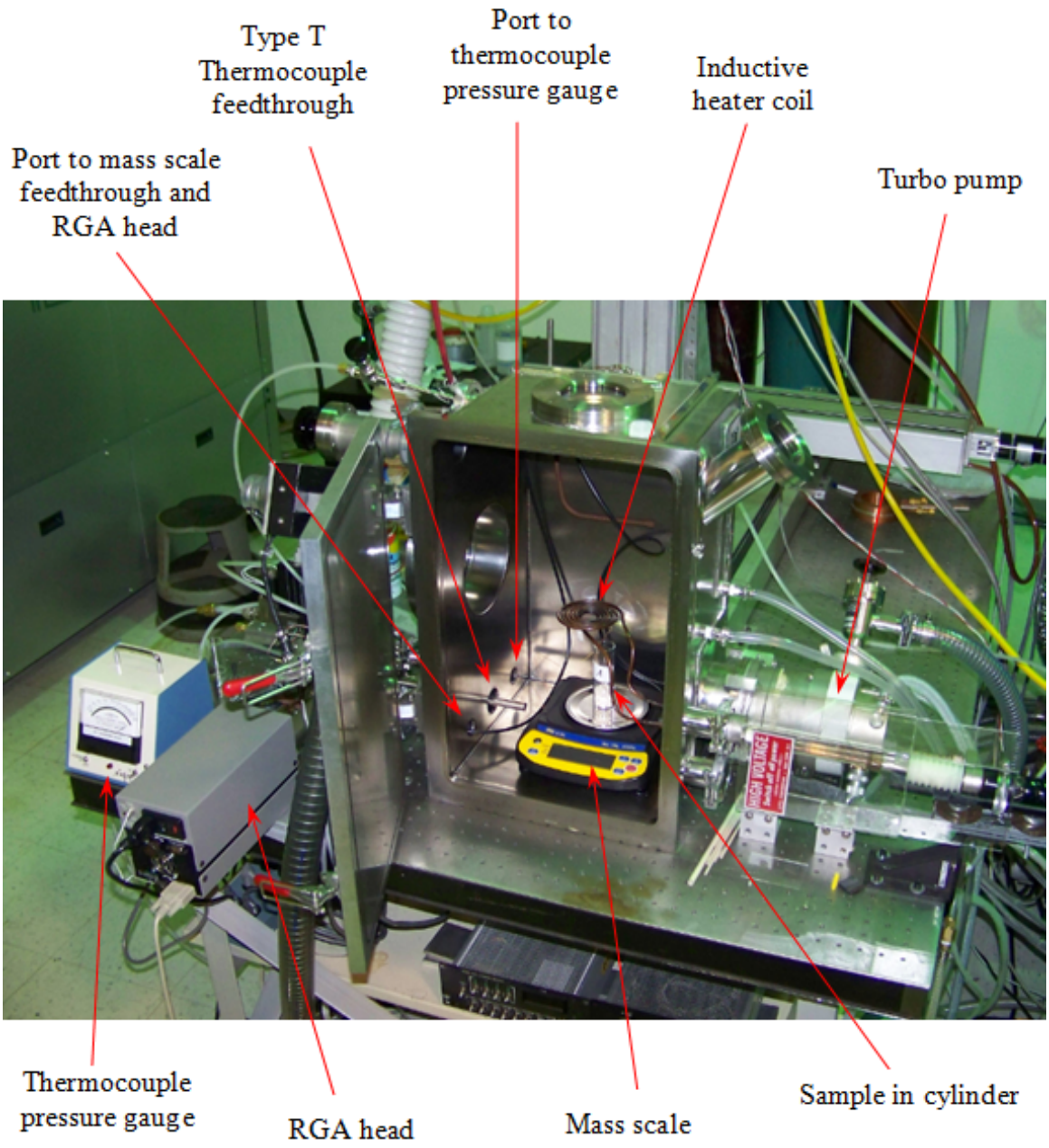

Figure 2.1: Vacuum chamber in the CLA at UTSI used for testing water source materials.

2.2 RGA100 overview

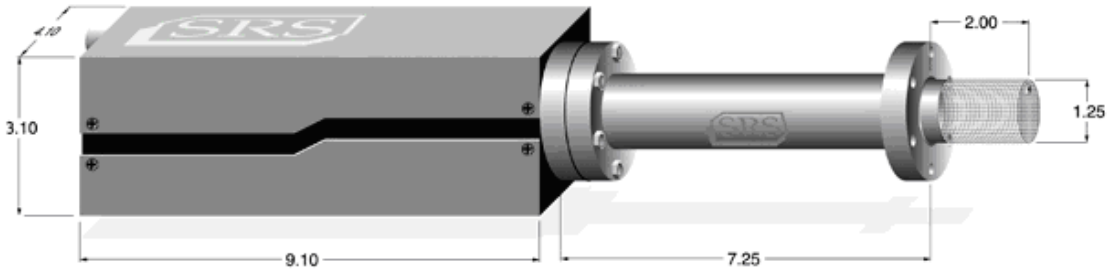

Figure 2.2: Stanford Research Systems RGA100 [5].

Figure 2.2 shows the RGA that was used for all the tests in this thesis. The SRS RGA100 has a mass range of 1 to 100 [amu] and resolution of 0.5 [amu] [5]. The RGA comes with its own analysis software that can be used to log and display analog scans of the spectrum of gases inside the chamber and keep track of their partial pressures as time passes. However, these analog scans can be misleading without a proper understanding of how the RGA works. According to the RGA manual, "The electron impact type of ionizer used in modern RGAs almost always causes more than one kind of ion to be produced from a single type of gas molecule. Multiple ionization, molecular fragmentation and changes in the isotopic composition of the molecule are responsible for this effect. All ions formed contribute to the mass spectrum of the molecule and define its fragmentation pattern." and "The identification and interpretation of mass spectra must begin with a knowledge and understanding of the standard fragment patterns of atoms and molecules that may exist in the system" [37]. In other words, some of the molecules that the RGA detects might not actually be present inside the vacuum chamber, but instead might be part of the fragmentation pattern of another molecule. For example, the fragmentation pattern for water is given in Figure 2.3.

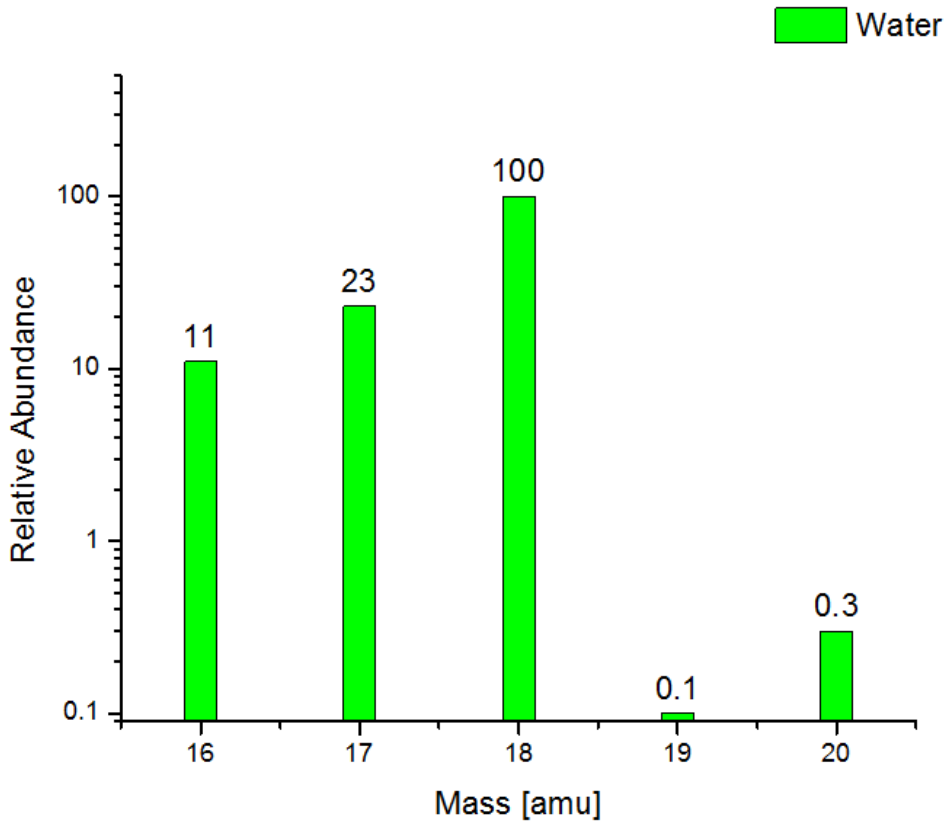

Figure 2.3: Fragmentation pattern of water.

Even though water is a single molecule of mass = 18 [amu], peaks at mass = 16, 17, 19 and 20 [amu] appear in its fragmentation pattern because of the way water molecules interact with the RGA. This is not too much of a problem though, because the RGA software comes with a tool that uses a library of standard fragmentation patterns to analyze the spectrum of gases that the RGA detects and determines what gases are actually present inside the chamber.

2.3 Basic pump down test setup

For these tests, samples were put inside a 3.75" tall, 1.25" O.D. glass cylinder and put in the vacuum chamber. The chamber was pumped down, and the RGA was used to analyze the spectrum of molecules in the chamber. Sample masses were measured with the electronic balance before and after pump down to see how their mass changed from being under vacuum.

2.4 Heating test setup

For these tests, samples were put inside an aluminum dish that was placed on top of an aluminum plate. The plate was positioned on top of another ceramic plate that electrically insulated it from the coils of the inductive heater that is driven by a Lepel 25.4 kVA, 60 Hz A.C. power supply. To heat the samples, A.C. power was sent to the heater which induced eddy currents inside the aluminum plate and the dish to heat them up. This heated the samples, and a thermocouple was pressed against the side of the aluminum dish to measure its temperature. A schematic of this setup with a photograph of the aluminum dish on top of the inductive heater is shown in Figure 2.4. The RGA was also used for these tests to measure the relative abundance of the different gases in the chamber.

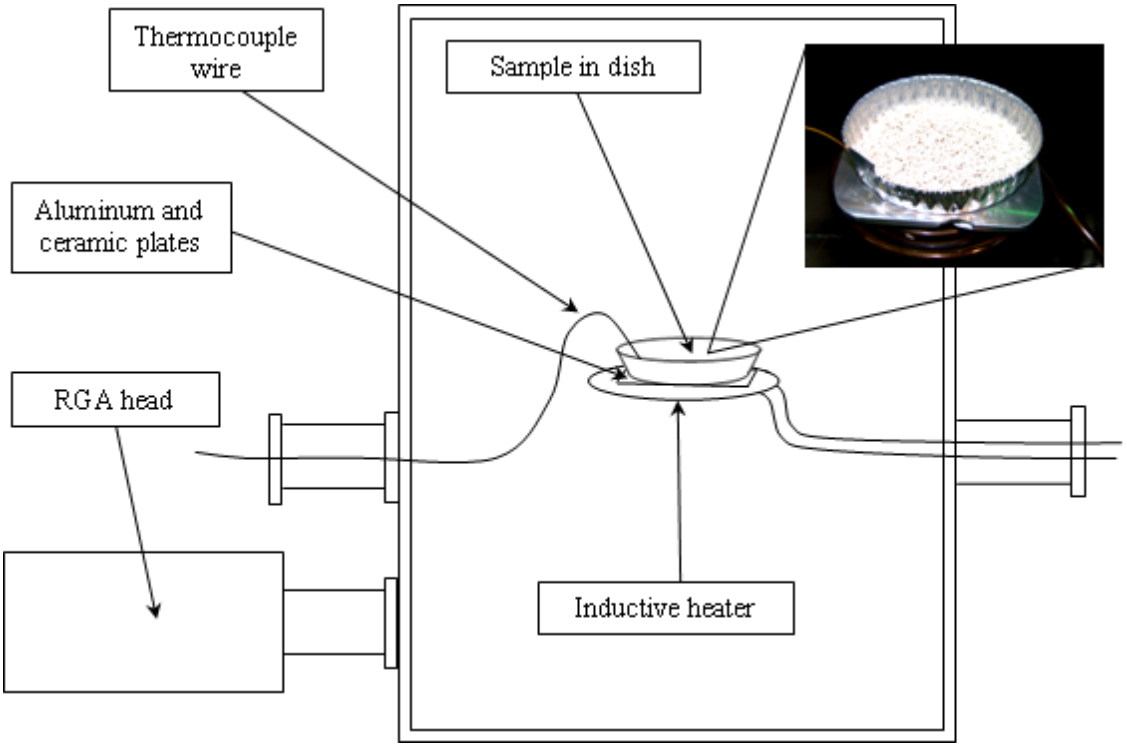

Figure 2.4: Chamber configuration for the heating tests with a picture of the samples in a dish on top of the inductive heater.

2.5 Dynamic mass change test setup

Samples were placed on top of the electronic balance inside the chamber that sent real time mass measurements to a computer while the chamber was in operation. The thermocouple and the RGA were both used for these tests as well. A schematic of this chamber configuration is given in Figure 2.5.

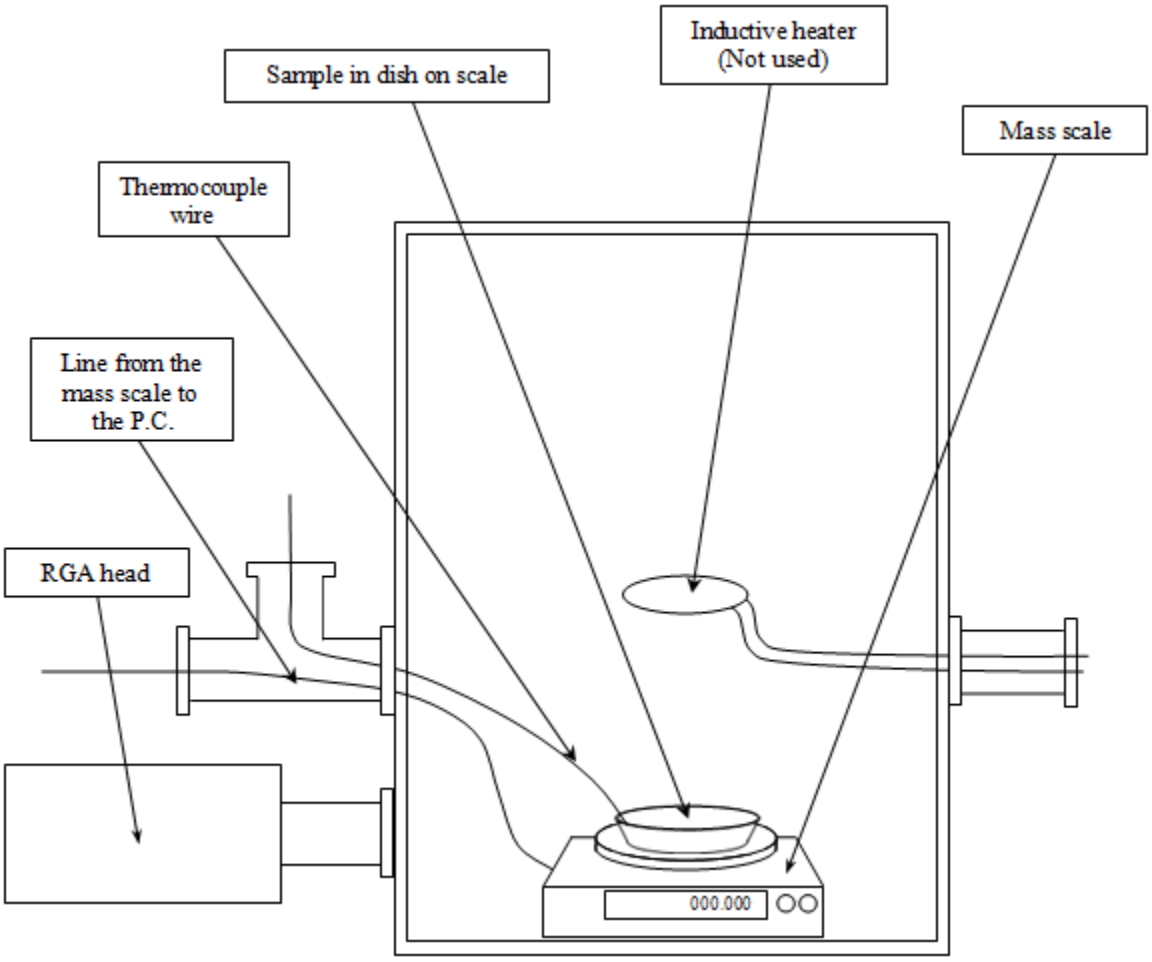

Figure 2.5: Chamber configuration for the dynamic mass change tests.

2.6 External chamber test setup

A schematic of the external chamber assembly is given in Figure 2.6. The external chamber is a combination of several different vacuum flanges, tubes and valves connected together. Together they have a total internal volume of about 70 in^3. The external assembly was connected to the main vacuum chamber by a 5/8" I.D. vacuum line that fed into the side of the main vacuum chamber. The vacuum line was attached to a valve on the external assembly that controlled the flow of gases to the main chamber. This allowed the main chamber to be pumped down while the external chamber assembly remained at atmospheric pressure. The other end of the external chamber was connected to a standard thermocouple pressure gauge and a leak valve. The thermocouple pressure gauge was used to measure the pressure in the external chamber while the RGA wais used to measure the pressure of the different gases inside main chamber. The leak valve was used to leak air into the external chamber so it could be opened up to change samples without having to open up the main chamber.

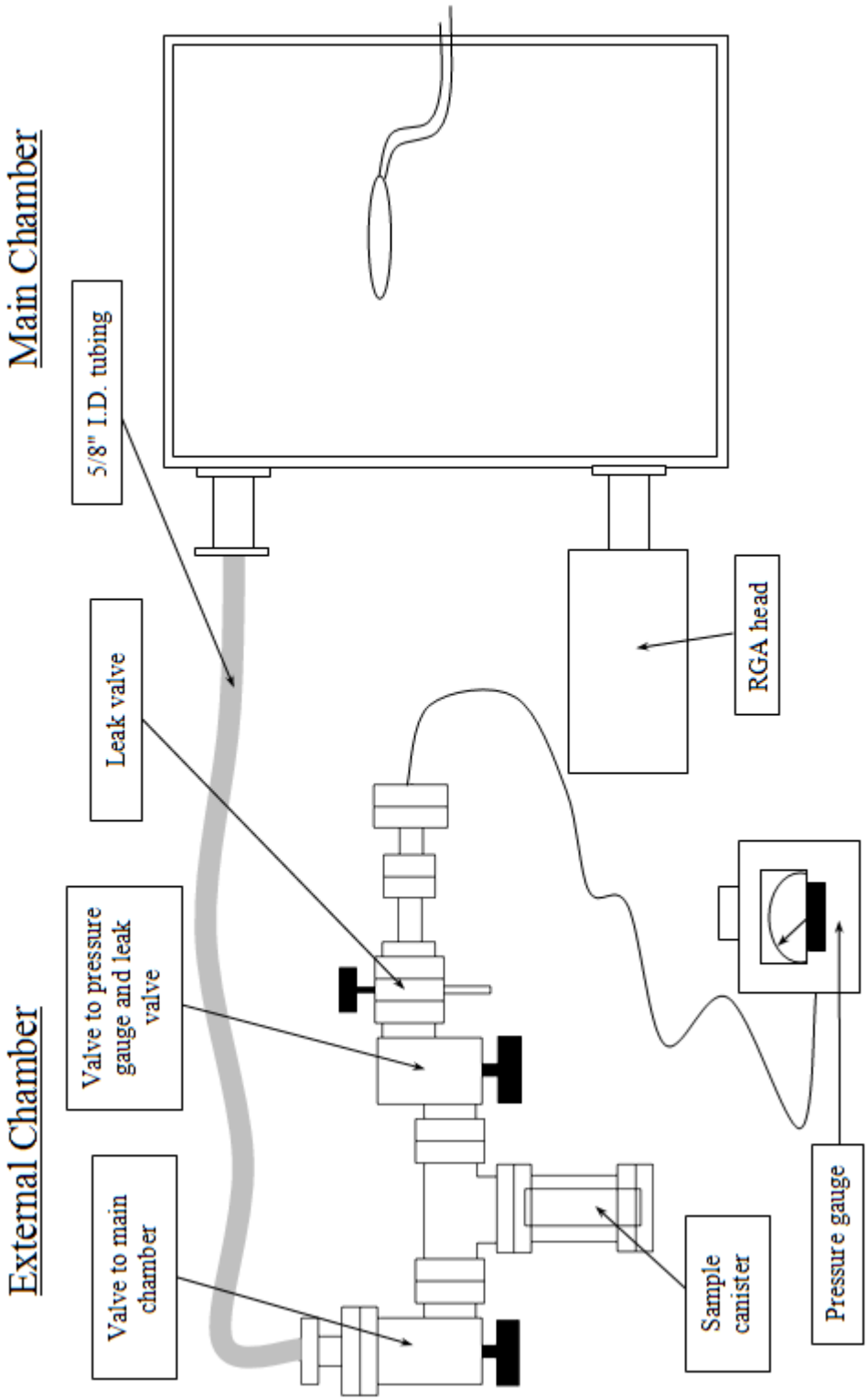

Figure 2.6: Configuration for the external chamber tests.

Chapter 3

Experimental proceedings

The following sections describe the goals, methods, and findings of each test.

3.1 Basic pump down tests

Basic pump down tests were run with the vacuum chamber empty and with small samples of calcium sulfate, cobalt chloride or the molecular sieves in the chamber. The empty chamber test was run to measure the background of gases inside the vacuum chamber, and the other tests were run to see what gases would come from the different samples inside the chamber. The masses of samples were measured before and after pump down to determining how the mass of each sample changed (if any) from being exposed to high vacuum ($\sim 10^{-6}$ torr).

3.1.1 Empty chamber

Virtually every vacuum system will have detectable amounts of hydrogen (2 amu), water (18 amu), carbon monoxide (28 amu) and carbon dioxide (44 amu) [5], but the chamber at the CLA has been used for many different types of experiments, and it could be much dirtier than most other vacuum systems. Tests were conducted to study the chamber during pump down and to measure its background gases. To do this, analog scans were taken with the RGA to measure the spectrum of gases present in the empty chamber while it was being pumped down.

The empty chamber was pumped down for approximately 24 hours, after which it reached a base pressure of about $3.3 \cdot 10^{-6}$ torr. That is comparable to pressures reached in the vacuum chamber at AEDC used for the cryodeposition tests. The RGA took analog scans at various points during the tests, and the scans shown in Figure 3.1 were taken approximately 15 min, 1 hr, 2 hrs, and 24 hrs after pump down started. Table 3.1 provides the spectrum analysis of those scans.

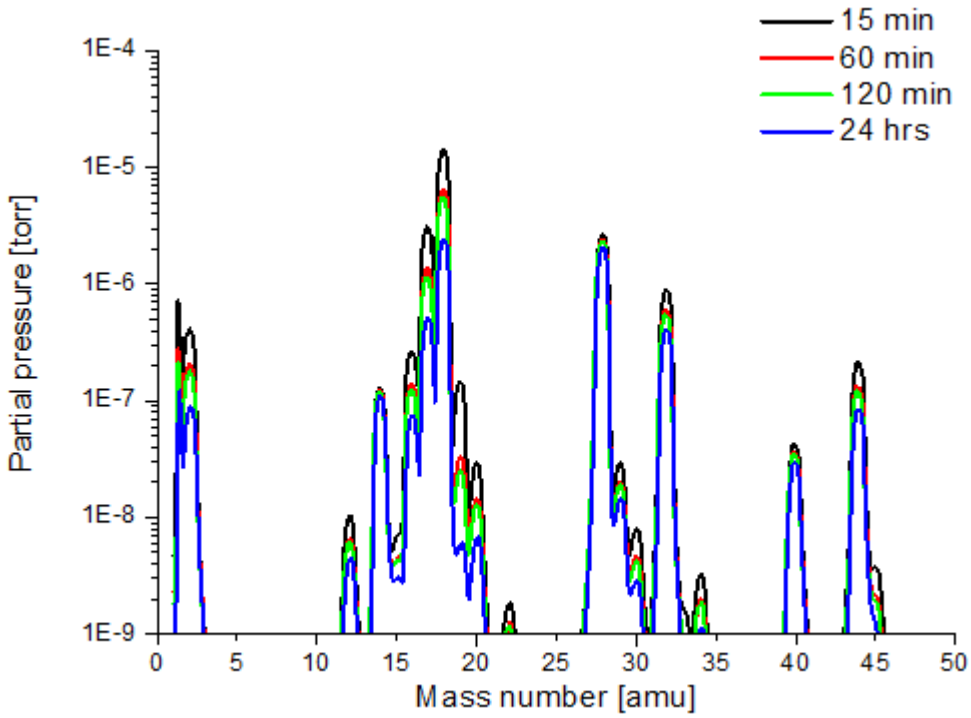

Figure 3.1: Analog scans from the empty chamber tests.

Empty Chamber	15 [min]	60 [min]	120 [min]	24 [hr]
Carbon dioxide	0.80%	1.10%	1.20%	1.50%
Hydrogen	1.80%	1.80%	1.70%	1.50%
Nitrogen	11.90%	20.80%	23.20%	36.00%
Oxygen	3.80%	5.20%	5.40%	7.10%
Water	81.60%	71.10%	68.50%	53.80%

Table 3.1: Spectrum analysis from the empty chamber test.

The most notable peaks are the ones with mass = 2, 14, 16, 17, 18, 19, 20, 28, 32, 40 and 44 amu. The gases with mass 16-20 amu are associated with water and its fragmentaion pattern. The mass = 2, 14, 28, 32, 40 and 44 amu gases are believed to be He , N, N_2, O_2, Ar and CO_2 respectivly. The m=2 could only be H_2. The m = 28 gas could be CO or N_2 but is most likely diatomic nitrogen, N_2, since it is very abundant and CO is usually only found in trace amounts in the atmosphere [38]. The m = 44 gas could be CO_2 or N_2O, but it is most likely CO_2 since it is supposed to be almost 1300x more abundant in the air than N_2O [38]. The RGA software was also used to track and log the partial pressures of ten gases at a time, which made it easier to track the relative abundances of a few specific gases in the chamber. Figure 3.2 shows the partial pressure of the gases with mass = 2, 14, 16, 17, 18, 28, 32, 40 and 44 [amu] throughout the entire test.

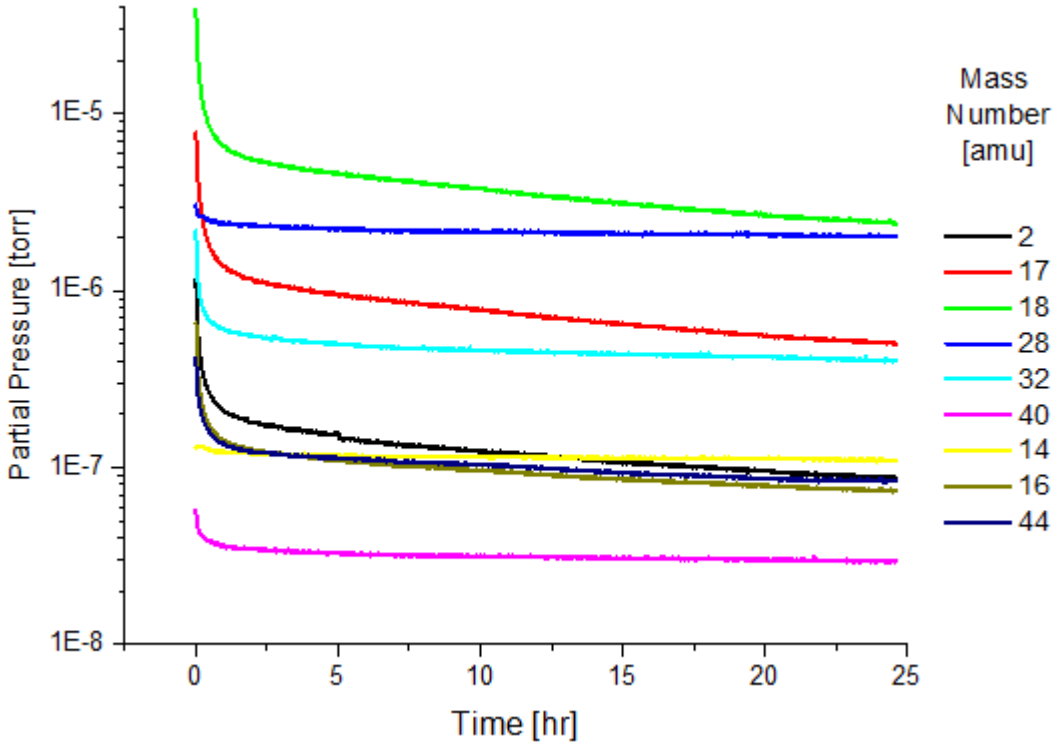

Figure 3.2: Partial pressure of various gases throughout the empty chamber test.

This chart shows that most of the gases in the chamber appear to be pumped out relatively quickly during the first 150 minutes, but they reach some sort of baseline and are pumped out much more slowly after that. This chart shows that the gas with m = 18 (water) was the most abundant gas in the chamber throughout the entire test. At the start of the test, the gas with m = 17 (part of the fragmentation pattern of water) was the second most abundant, but as time passed, it was surpassed by a gas with m = 28 (N_2). Ultimately, this data provides a baseline to which the results from the following basic pump down tests can be compared.

3.1.2 Calcium sulfate dihydrate

The same type of test was repeated with a small amount of calcium sulfate inside the chamber to see what kinds of gases it released when it was exposed to a vacuum. Comparing the analog scans taken during this test to the analog scans taken during the empty chamber test should reveal which gases (if any) would come from the calcium sulfate.

A 4.82 g sample of calcium sulfate powder was placed inside a 3.75" tall, 1.25" O.D. glass cylinder and put inside the chamber. The mass of the sample was measured before and after pump down to see how much it changed (if any) and to determine how much material it lost during pump down. The chamber was pumped down for approximately 24 hours and reached a base pressure of $4.7 \cdot 10^{-6}$ torr. The mass of the sample decreased from 4.82 g down to 4.25 g, an 11.8% mass loss, without any heating, just from being exposed to vacuum conditions. Analog scans taken at 20 min, 60 min, 120 min and 24 hrs after pump down are given in Figure 3.3 and the spectrum analysis of those scans are given in Table 3.2.

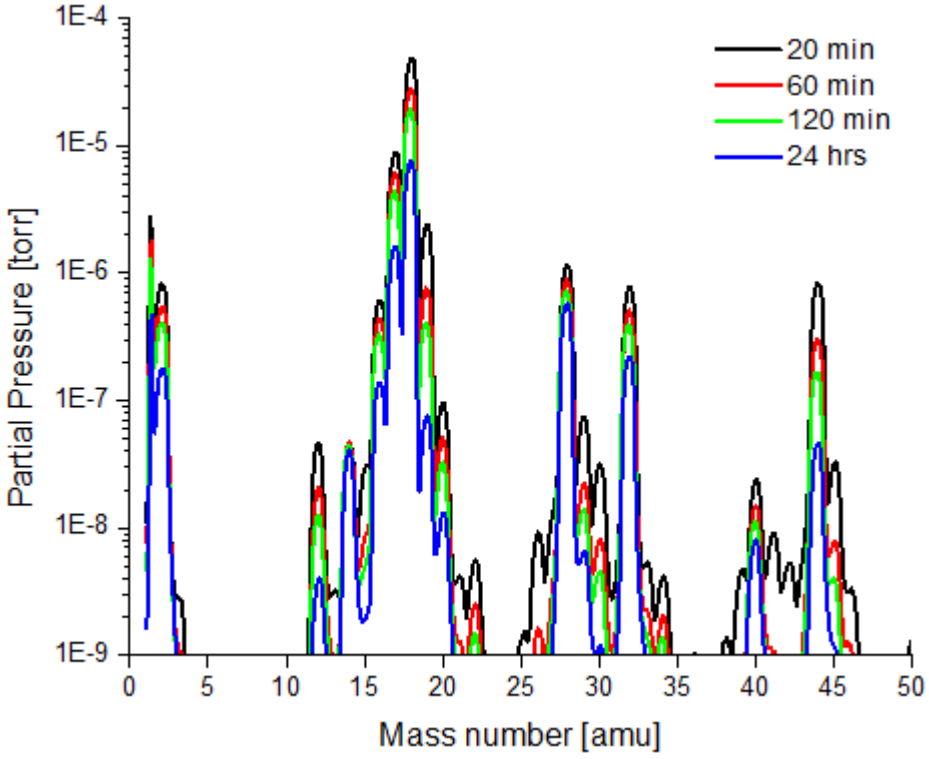

Figure 3.3: Analog scans from the calcium sulfate test.

Calcium Sulfate	19 [min]	60 [min]	120 [min]	24 [hr]
Carbon dioxide	1.20%	0.60%	0.30%	0.10%
Hydrogen	1.30%	1.40%	1.50%	1.60%
Nitrogen	1.70%	2.20%	2.70%	5.50%
Oxygen	0.90%	0.90%	1.00%	1.80%
Water	94.90%	94.80%	94.40%	91.00%

Table 3.2: Spectrum analysis from the calcium sulfate test.

The analog scans are similar to the ones taken during the empty chamber test, but a greater amount of water vapor was present with the calcium sulfate in the chamber than there was when the chamber was empty (94.8% versus 71.1% at 60 min). This can be seen by comparing the partial pressure of water as a function of time for each test as seen in Figure 3.4.

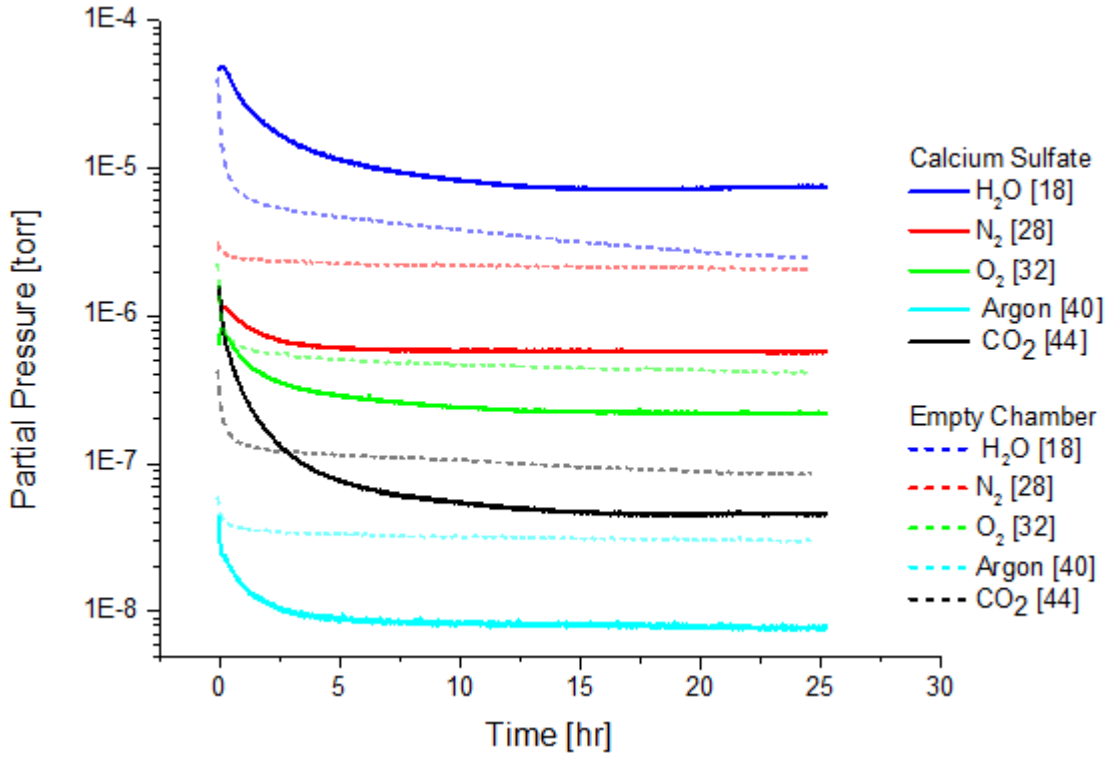

Figure 3.4: Comparisons of the partial pressure of various gases inside the vacuum chamber for the calcium sulfate test.

These plots and the mass loss that was observed suggest that calcium sulfate started to lose some of its water during pumpdown without any heating. The recorded mass loss was 11.8%, which was only slightly lower than the range of the expected maximum mass loss, 13.7%-16.5%. It is possible that the calcium sulfate had, in some capacity, adsorbed some additional water on its surface. But since the mass loss was so high, it is more likely that, while under vacuum, the ambient room temperatures were high enough to break the bonds between the water molecules to start dehydrating the calcium sulfate dihydrate.

3.1.3 Cobalt(II) chloride hexahydrate

As before, this test was run to see how the cobalt chloride would behave when it was exposed to a vacuum, and to see what kind of gases it would release. To prepare the sample, a small amount of dark red cobalt chloride was ground up into a fine powder. A photograph of a ground sample next to an un-ground sample is given in Figure 3.5.

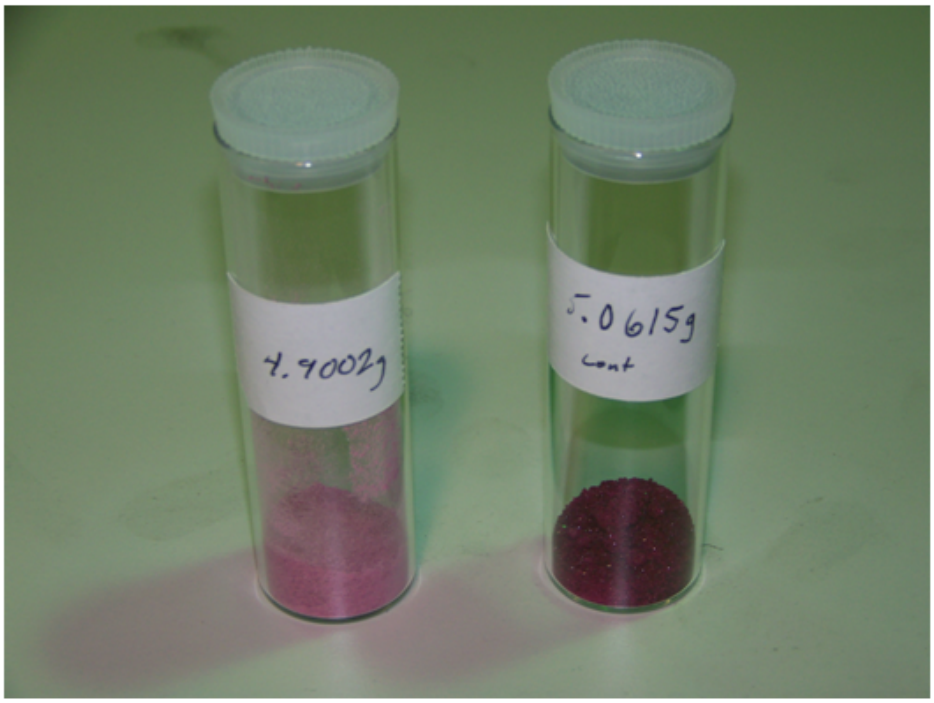

Figure 3.5: Ground (left) and un-ground (right) samples of hydrated cobalt chloride.

4.83 grams of the ground sample was put inside the vacuum chamber and pumped down for approximately 25 hours. Something happened during the test that caused the RGA to fail after about 16.75 hrs of pump down. After the test was over, the chamber was opened and cobalt chloride powder was found all over the chamber. Most of the sample had changed from light red to a light purple color and some of it changed to a very distinct blue, indicating that at least part of the dehydration process had taken place. This can be seen in the photograph in Figure 3.6. The mass of the sample changed from 4.83 grams to 4.30 grams, nearly an 11.0% decrease, but this measurement is not to be considered very accurate since some of the sample was lost when it was blown out of its container.

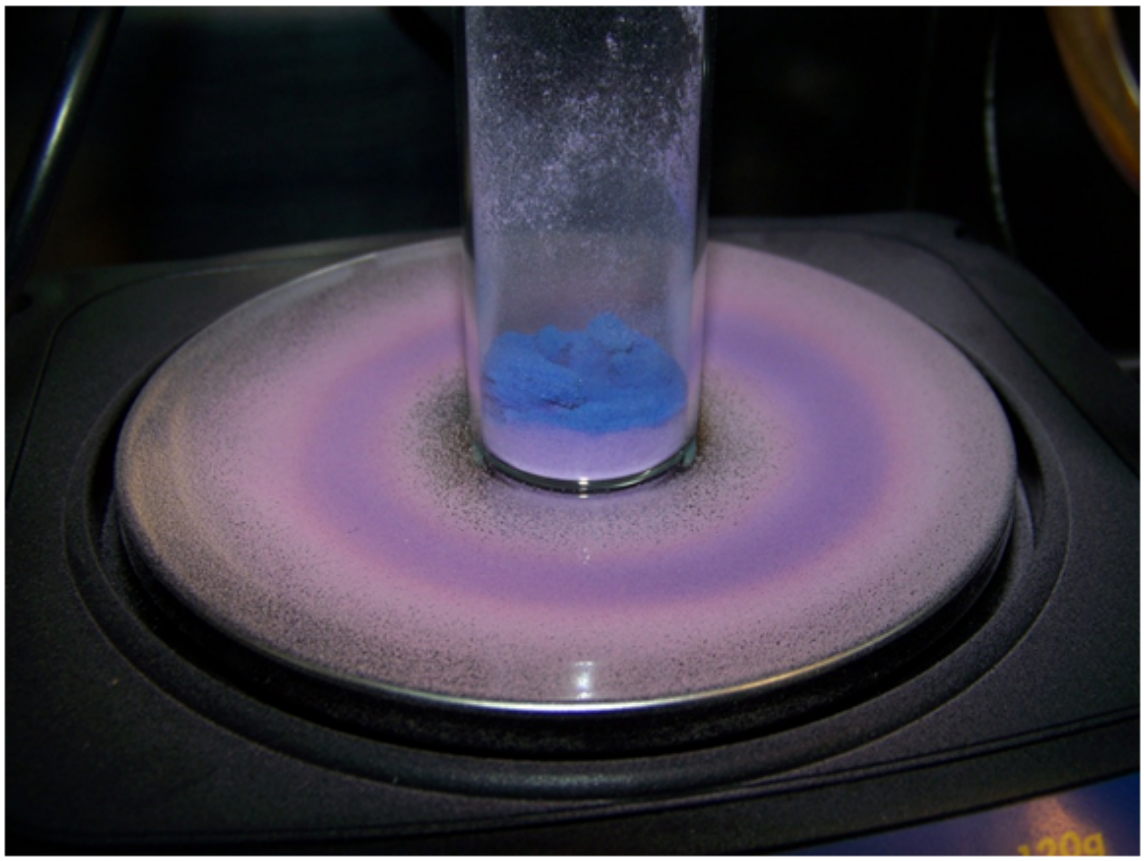

Figure 3.6: Cobalt chloride powder blown out of a glass cylinder and color variation after a basic pump down test.

The test was repeated later with a 3.03 gram sample inside the same glass cylinder, but this time the cylinder had a cap with a 3mm diameter hole drilled in the top of it. The test lasted 24 hours and the chamber reached a base pressure of $4.9{\cdot}10^{-6}$ torr. The mass of the sample decreased from 3.03 grams to 2.78 grams, an 8.25% mass loss. Analog scans taken at 23 min, 60 min, 120 min and 24 hrs are given in Figure 3.7, and the spectum analyis of those scans are given in Table 3.3.

These scans show similar trends and peaks to those seen in the analog scans from the empty chamber and calcium sulfate tests. Again, there was a greater amount of water in the chamber than there was for the empty chamber test (95.0% versus 71.1% at 60 min), and there does not appear to be a greater amount of any unusual gases in the chamber either.

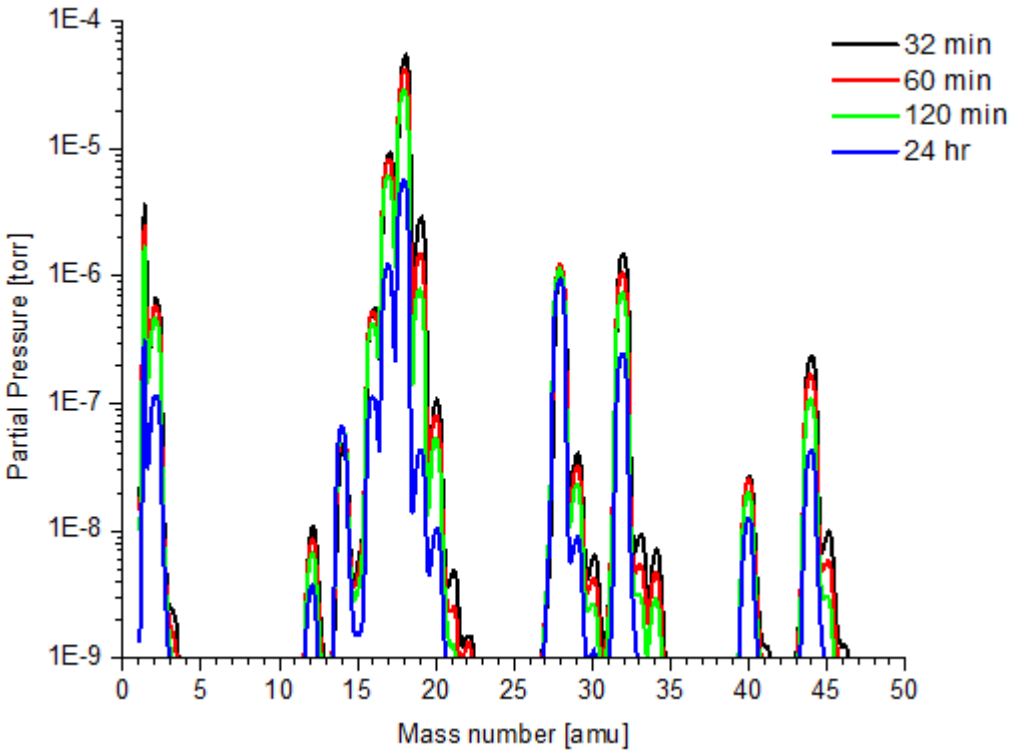

Figure 3.7: Analog scans from the cobalt chloride test.

Cobalt(II) Chloride	23 [min]	60 [min]	120 [min]	24 [hr]
Carbon dioxide	0.10%	0.00%	0.00%	0.20%
Hydrogen	0.90%	1.00%	1.20%	1.30%
Nitrogen	1.40%	2.30%	3.00%	11.00%
Oxygen	1.80%	1.60%	1.50%	2.60%
Water	95.70%	95.00%	94.30%	84.90%

Table 3.3: Spectrum analysis from the cobalt chloride test.

The partial pressure versus time plot given in Figure 3.8 shows a peak in the partial pressure water vapor during the first hour of the test followed by a steady decrease in partial pressure after that. At about hour 19, the partial pressure of water vapor appears to drop more rapidly than it did before. The cause for this is yet to be determined. The partial pressure of the other gases all appear to have been behaving in a manner that was somewhat similar to the behavior of the water vapor. However, the CO_2 appears to have

been increasing slightly in between hours 16 and 19, and the partial pressure of N_2 appears to have been increasing rapidly at the beginning of the tests, and then decreasing only a little bit after that. This sort of trend seen for N_2 is not characteristic of outgassing from a finite source inside the vacuum chamber like the one seen for water vapor and the other gases. It is instead more like outgassing from an infinite source outside the vacuum chamber, which is indicative of a leak somewhere in the chamber [39]. It's not clear wheather the other gases (O_2, CO_2 and argon) were coming from the cobalt chloride or if they were behaving differently because of some effect that the increased amount of water vapor in the chamber had on the rate at which these other gases are pumped out of the chamber.

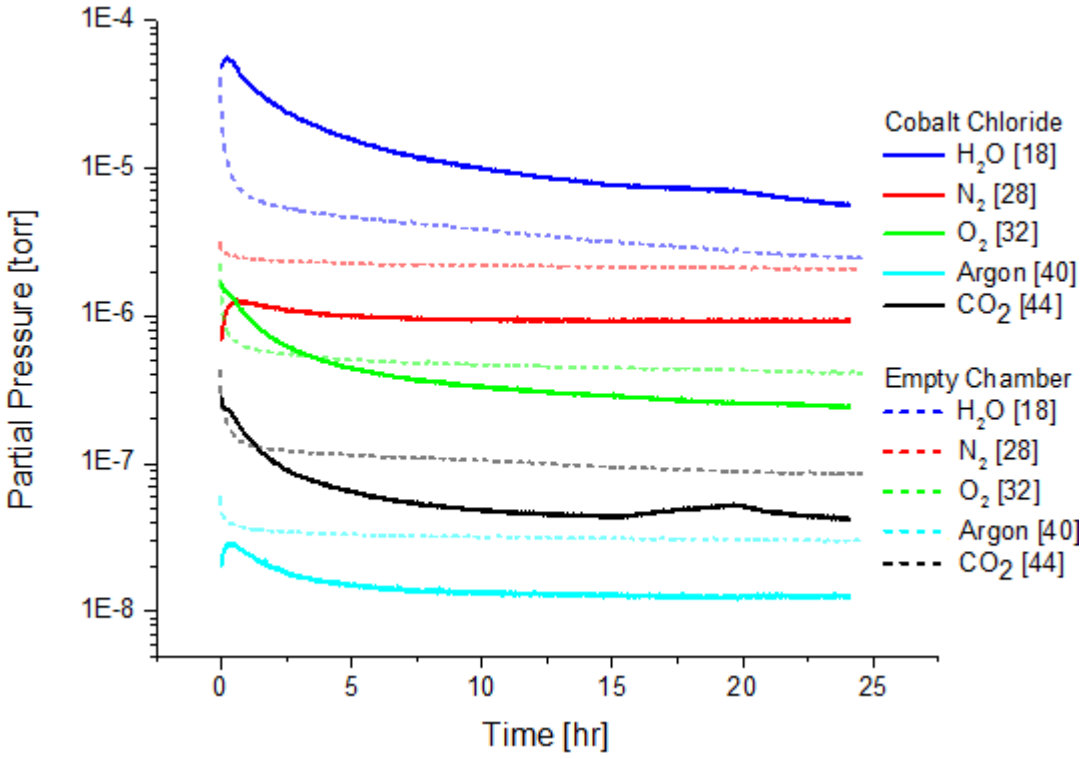

Figure 3.8: Comparisons of the partial pressure of various gases inside the vacuum chamber for the cobalt chloride test.

These tests revealed some serious problems associated with the cobalt chloride. Not only would there be problems keeping the material contained within the effusion cell, the color change during pump down definitively showed that the cobalt chloride would release

its water at room temperature in the vacuum. That meant that the cobalt chloride could potentially lose all of its water during pump down, before any heating had started and before the test was ready to begin. The cobalt chloride also seemed to react with and corrode some of the aluminum dishes that it came in contact with. This reaction could potentially damage the effusion cell since it was made entirely out of aluminum.

3.1.4 Zeolite molecular sieves

For these tests, an 11.95 g sample of 3Å K type zeolite molecular sieves was placed in a tall glass cylinder, and just as before, it was put inside the chamber to see how it would behave when exposed to a vacuum and to see what kind of gases (if any) it would release. A photograph of some KA type zeolite samples inside some of the glass cylinders is given in Figure 3.9. As before, the mass of the sample was measured before and after pump down, and analog scans were taken with the RGA throughout the test. The analog scans were used to determine what gases would be outgassed from the zeolite, and the mass measurements were used to see how much water (if any) it would lose during pump down.

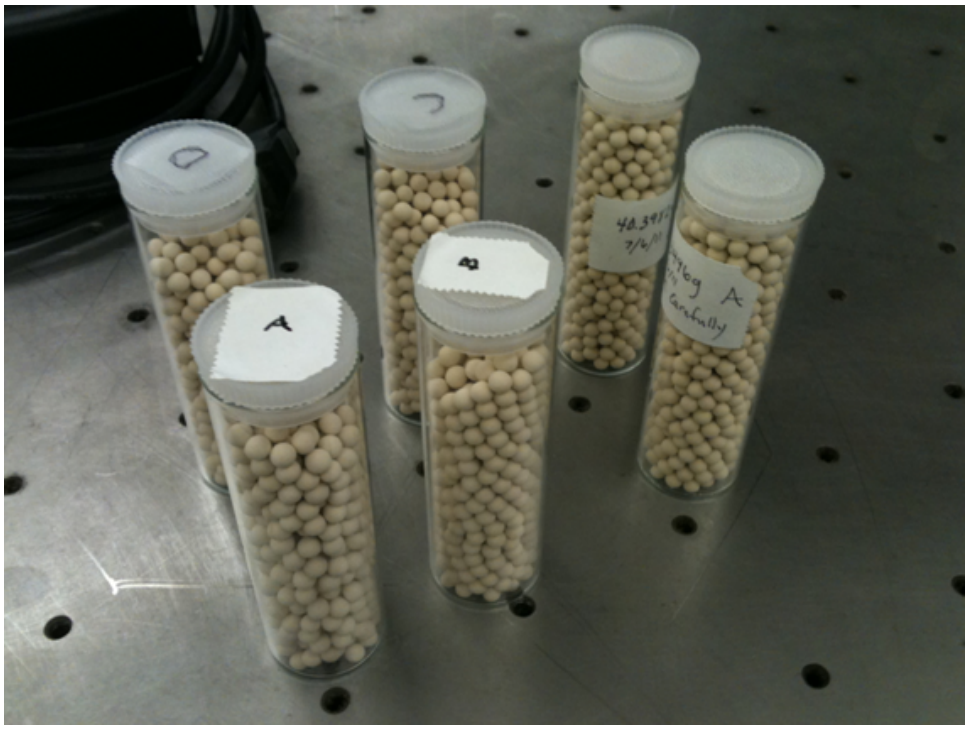

Figure 3.9: Photograph of 3Å K type zeolite molecular sieves.

The sample was pumped down in the vacuum chamber for about 24 hours, after which the base pressure was measured to be $3.8 \cdot 10^{-6}$ torr. The mass of the zeolite had decreased from 11.95 g down to 10.16 g, a 15.0% decrease. Analog scans taken at 30 min, 60 min, 120 min and 24 hrs after pump down are given in Figure 3.10. The spectrum analyses of those scans are given in Table 3.4.

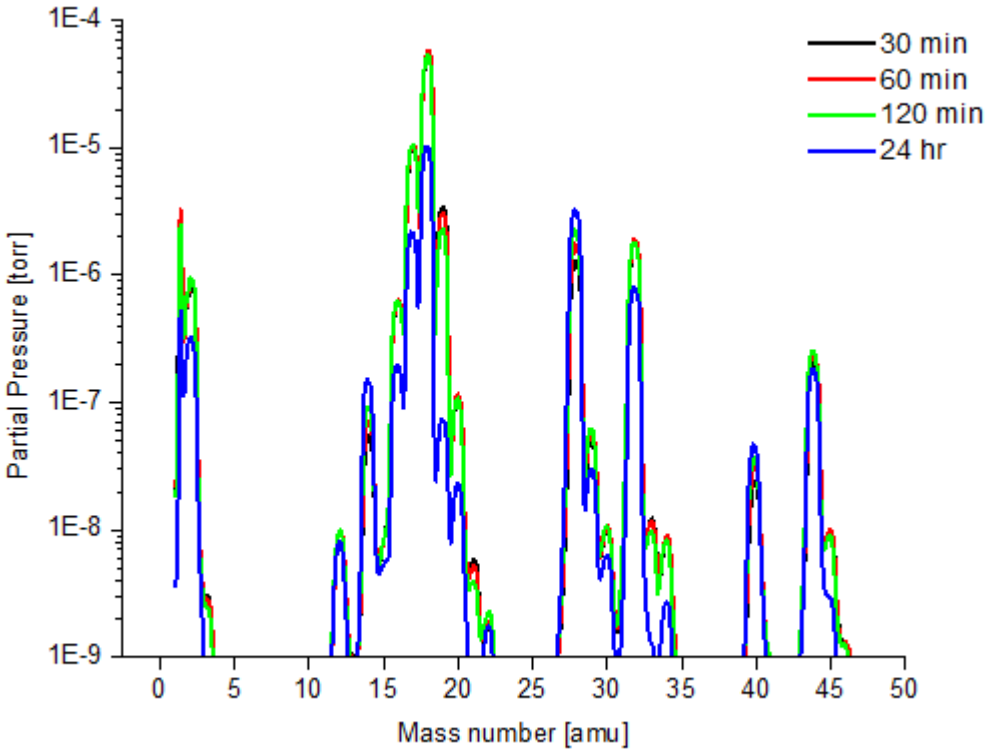

Figure 3.10: Analog scan from zeolite test.

Zeolite	30 [min]	60 [min]	120 [min]	24 [hr]
Carbon dioxide	0.10%	0.10%	0.10%	0.90%
Hydrogen	1.10%	1.20%	1.30%	1.80%
Nitrogen	1.80%	2.30%	3.20%	18.80%
Oxygen	2.20%	2.30%	2.20%	4.40%
Water	94.80%	94.20%	93.30%	74.00%

Table 3.4: Spectrum analysis from the zeolite test.

The analog scans and spectrum analyses are similar to the ones from the other tests, and they also show no unusual species coming from the zeolite. These scans show an increased amount of water vapor in the chamber compared to the empty chamber test (94.2% versus 71.1% at 60 min). However, water was not the only gas that was behaving differently. The partial pressure of N_2 and argon (m = 28 and 40 amu) seemed to have been increasing throughout the test. The data in Figure 3.11 show this more directly by plotting the partial pressure of these gases (and water vapor) against time throughout the zeolite and the empty chamber tests.

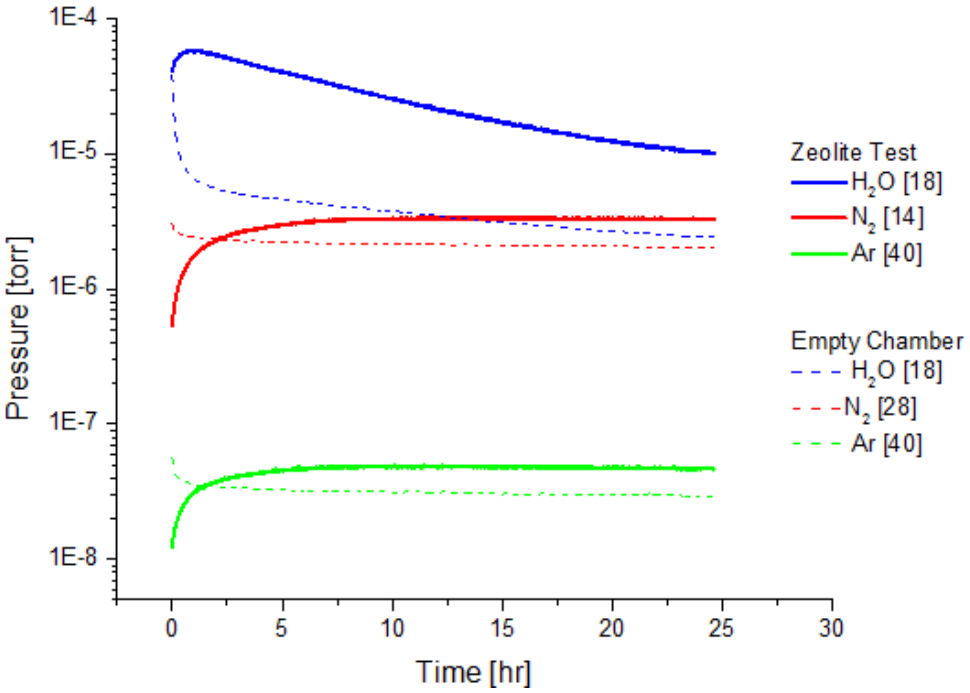

Figure 3.11: Comparisons of the partial pressure versus time trends of H_2O, N_2 and Ar for the empty chamber and the zeolite tests.

Clearly the partial pressure of water vapor was the greatest throughout the entire zeolite test, but the partial pressures of N_2 and argon grew asymptotically to nearly constant values. Again, this sort of trend is not characteristic of outgassing from a finite source inside the chamber like the trend seen for water vapor. This is instead more indicative of a some kind of virtual leak in the chamber [39]. So the N_2 and the Argon are not believed to be outgassed from the Zeolite.

There were a number of other gases that were behaving differently as well. Figure 3.12 shows the analog scans taken at 120 minutes for both the empty chamber and zeolite tests show the difference between the two cases more clearly.

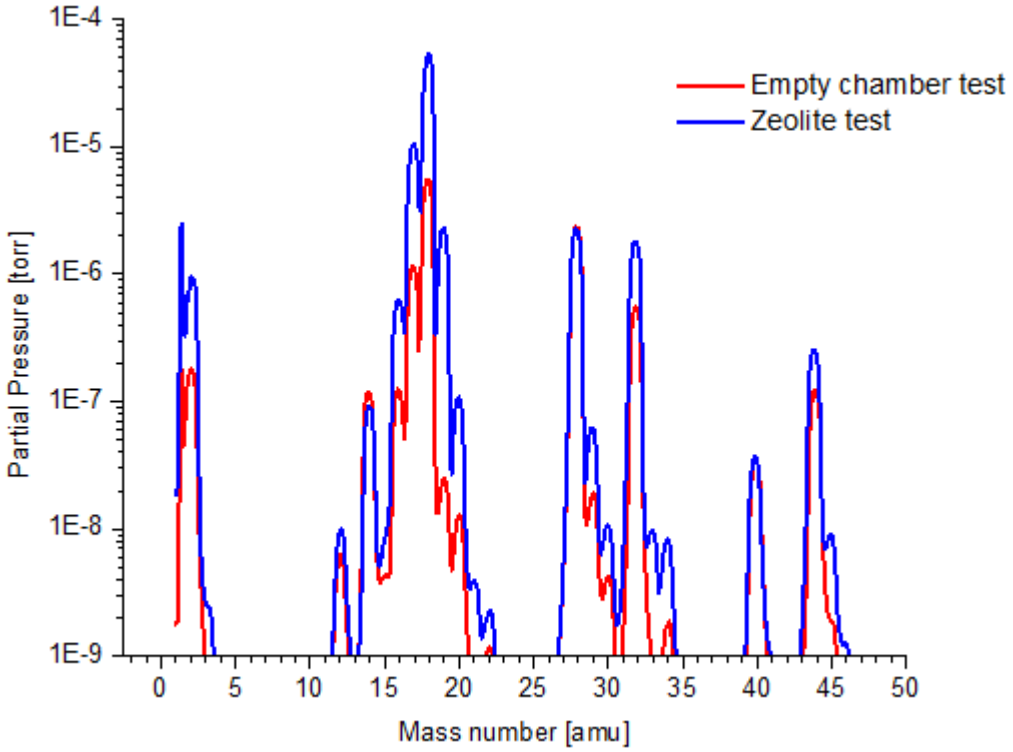

Figure 3.12: Analog scans taken at 120 min for the empty chamber and zeolite tests.

Figure 3.12 clearly shows differences in the abundance of several gases in the chamber. The most notable ones are those with mass = 2, 16, 17, 18, 19, 20, 32 and 44 amu. As before, many of these gases are associated with the fragmentation pattern of water(m = 16-20), but some of them are not (m = 2, 32, and 44). The plot in Figure 3.13 shows the partial pressure of the most significant gases, H_2O, H_2, O_2 and CO_2, throughout the zeolite and the empty chamber tests.

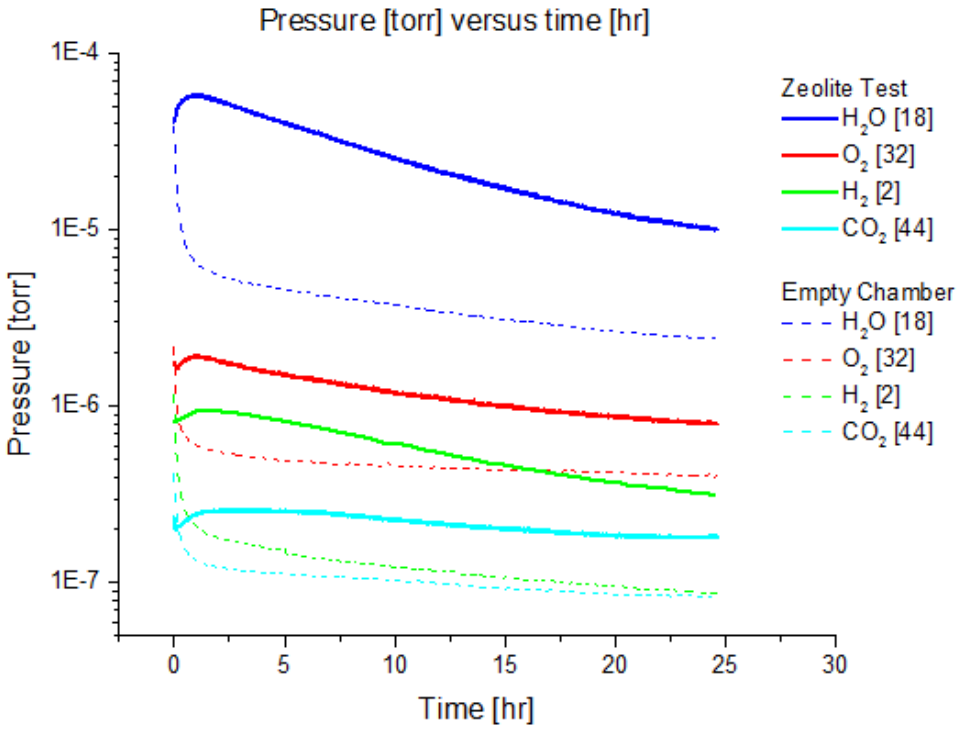

Figure 3.13: Comparisons of the partial pressure versus time trends of H_2O, O_2, H_2 and CO_2 for the empty chamber and the zeolite tests.

All of these gases follow the same general trend, and it appears that the zeolite could have been outgassing all of these gases. However, even if the zeolite does adsorbe and release all of these gases, it might not be a problem. The pressures in the chamber should not go below 10^{-7} torr for the cryodeposition tests, and the temperatures of the test surfaces are not expected to go below 40 K, which would be required to freeze H_2, N_2, Ar, O_2, CO and NO [40]. However, temperatures are expected to go below 80K, which would be cold enough to freeze CO_2 at 10^{-7} torr [40]. But since the partial pressure of CO_2 is 2 orders of magnitude lower than the partial pressure of water vapor, it might not be a very big problem either. Overall, the differences in partial pressures of these unwanted gases is very small when they are compared to the amount of water vapor that the zeolite provided. To illustrate this, Figure 3.14 combines plots of the partial pressures of all the gases in Figures 3.11 and 3.13 against time with a linear vertical pressure scale. Figure 3.14 clearly shows that the zeolite was predominately outgassing water, and that any other gases that it may have released were released in much smaller quantities.

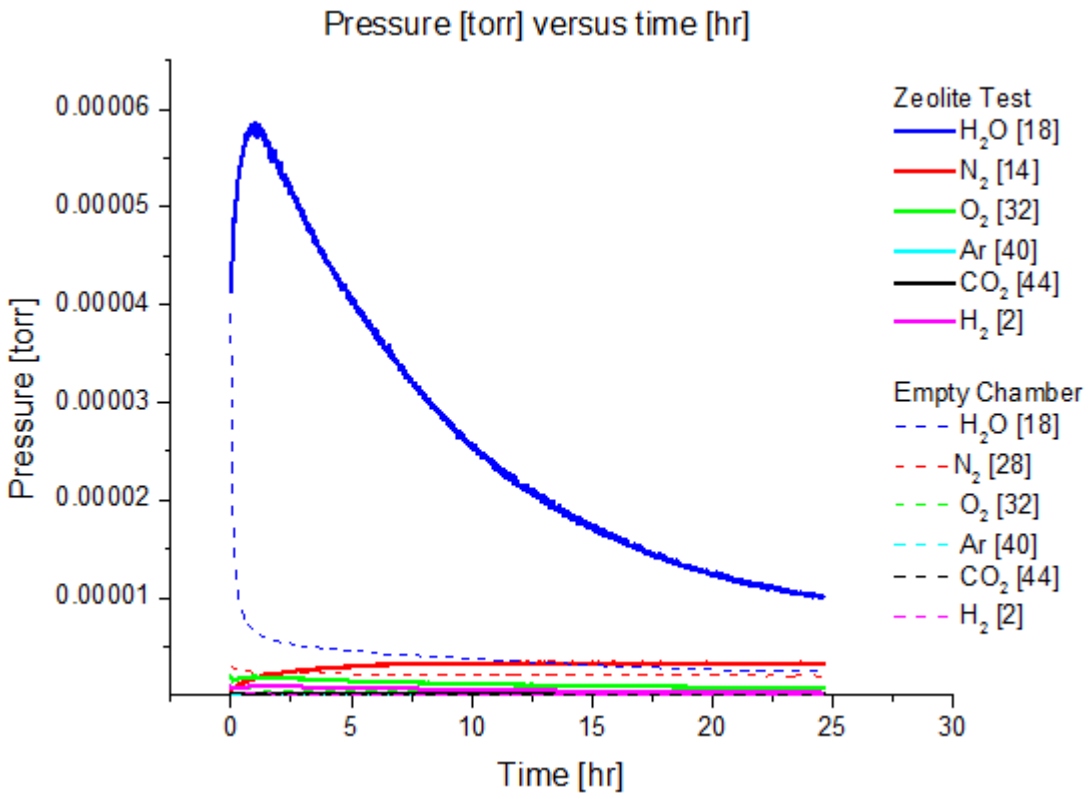

Figure 3.14: Comparisons of the partial pressures versus time of various gases versus time for the empty chamber and the zeolite tests.

To show how the zeolite compared to the calcium sulfate and the cobalt chloride, the partial pressure of water vapor and N_2 from all four tests are plotted versus time in Figure 3.15. That Figure shows a much greater amount of water vapor present in the chamber throughout the entire zeolite test than there was for any of the other tests, however this could be misleading since the zeolite sample was larger (almost 2x by mass) than the other samples were. This chart also shows that even though the partial pressure of a few other gases varied with each test, the differences were relatively small compared to the amount of water each material provided.

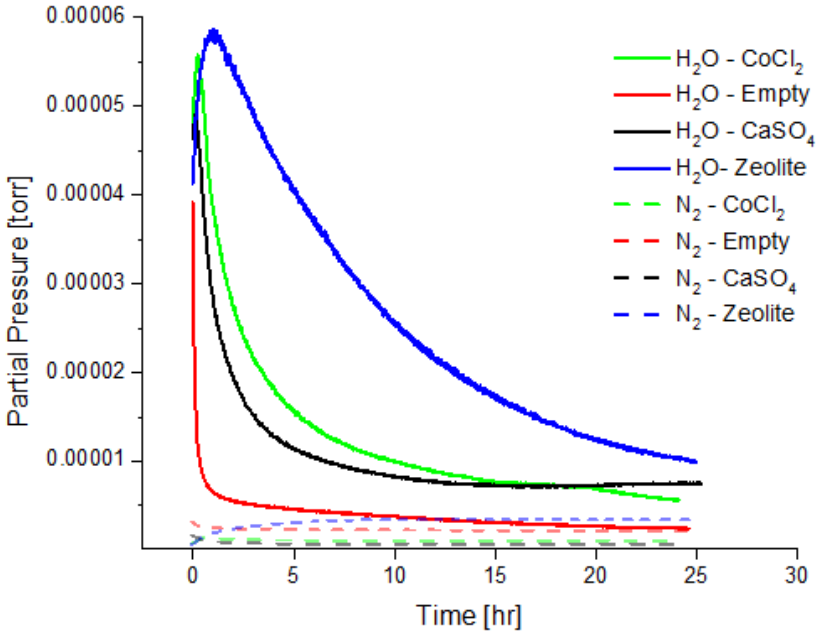

Figure 3.15: Comparisons of the partial pressure of water vapor and N_2 for all four tests.

3.1.5 Summary for the basic pump down tests

After these tests, the zeolite molecular sieves seemed to be the most suitable material for the cryodeposition tests. Even though the zeolite may outgas a small amount of materials other than water, it did not seem to be breaking down during the test, and it was not likely to be blown around during a cryo test like the calcium sulfate and the cobalt chloride were. Also, judging by Figure 1.4, it is possible that the KA type of zeolite might adsorb and release fewer unwanted contaminants than the NaA type did. All three materials proved capable of providing water vapor, but the zeolite comes in a nice beaded form, and these larger (∼4 mm diameter) and heavier (∼0.077 g) zeolite beads are much less likely to be blown around during pump down. This also makes the zeolite less hazardous than the other two materials, since it is much less likely to be inhaled or blown into someone's eyes. It is possible that the calcium sulfate and the colbat chloride could provide more water with some additional heating, but the zeolite is able to provide a sufficent amount of water vapor without any heating, and it could probably provide even more when heated. Therefore, instead of extensively studying all three candidates, it was decided to focus on the molecular sieves unless they were found to be othewise unfit.

3.2 Heating tests

These tests involved heating a sample of zeolite while it was in the vacuum chamber to determine the effect of heating. Samples were put in the chamber to see how the partial pressure of various gases changed as the sample was heated. These tests were also used to help further determine exactly which gases were coming from the zeolite. Since the heating would be applied directly to the zeolite, the partial pressures of any gases that it released should increase when it is heated.

An 11.94 g sample of 3Å NaA type zeolite was put in the vacuum chamber for about 39 hours and then it was heated for about 2.5 hours after that. The sample was in the vacuum chamber for almost 43 hours in total and reached a maximum temperature of 90.9°C. After the test, the mass had decreased from 11.94 g down to 10.39 g, for a mass loss of nearly 13.0%.

The partial pressure of the gases with mass = 18, 28, 32 and 44 amu (H_2O, N_2, O_2 and CO_2 respectively) were logged throughout the test. In retrospect, more gases, such as hydrogen and argon, should have been measured as well, but that was not clear at the time of these tests. Plots of their partial pressures throughout the tests are given with a logarithmic scale in Figure 3.16. The same data is plotted again with linear scale in Figure 3.17. These charts show the significance of each gas and how each was affected by the heating. Clearly, CO_2, O_2, and H_2O were released from the 3Å NaA type zeolite during heating while the N_2 was not affected.

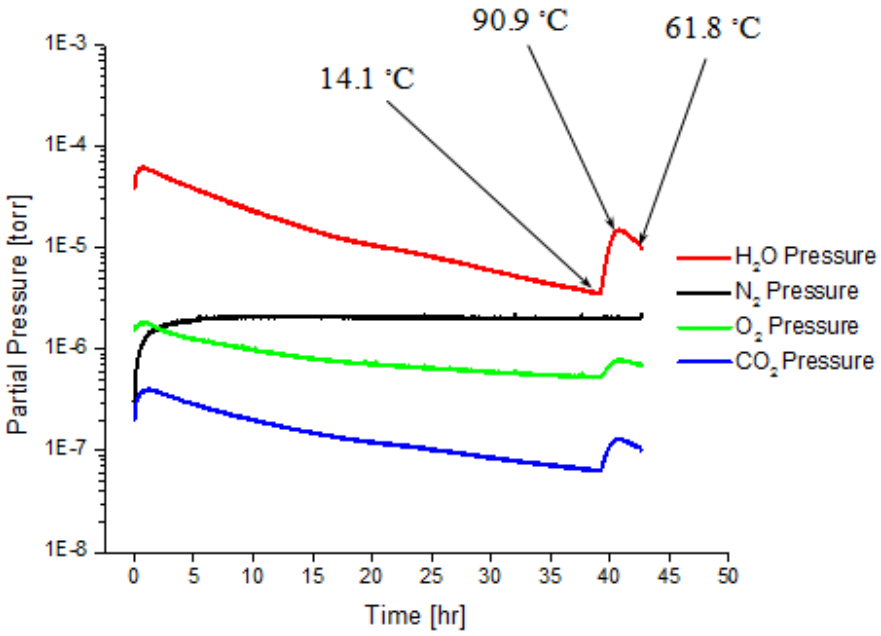

Figure 3.16: Partial pressure of water vapor, N_2, O_2, and CO_2 as a function of time during the heating test. Heating started after nearly 39 hours of pump down.

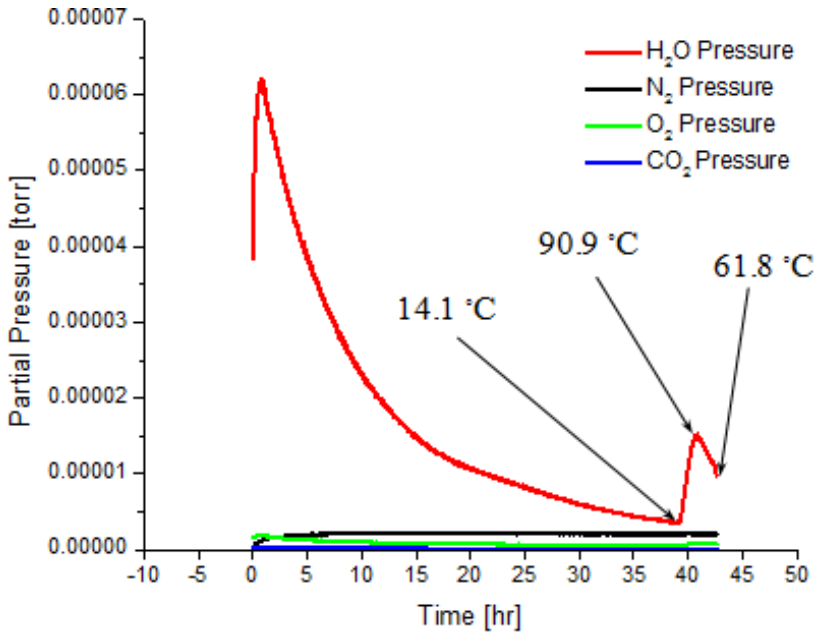

Figure 3.17: Partial pressure of water vapor, N_2, O_2, and CO_2 as a function of time during the heating test with a non logarithmic vertical scale.

Figures 3.16 and 3.17 show that the heating had a significant impact on the outgassing of water from the zeolite. Even after 39 hours of pump down, when the sample was believed to be nearly completely unsaturated, heating caused the partial pressure of water vapor in the chamber to increase. These charts also show that the zeolite might not have been outgassing any N_2 since its partial pressure did not increase when the zeolite was heated. However, the partial pressure of O_2 and CO_2 did increase, which meant that the NaA type zeolite was able to adsorb and release those gases; even though it was not releasing any N_2. O_2 and CO_2 molecules have a minimum kinetic diameters of 3.46Å and 3.3Å [4]; both are small enough to fit through the windows of 4Å molecular sieves, but both are non-polar and less likely to be adsorbed by the sieves than water is. This explains why trace amounts of these gases might be present in the zeolite. However, by the same logic, it is also possible that hydrogen and argon were also adsorbed by the zeolite, since both molecules are small enough (σ = 2.6Å and 3.40Å respectivly [4]) to fit through as well. The partial pressures of those gases were not logged throughout this test, so another test would have to be run to look at the partial pressures of hydrogen and argon to determine if they were being released or not too.

Another test was run for the same amount of time to compare the mass losses from a heating test to the mass losses from a test without heating. An 11.97 g sample was left in the vacuum chamber for approximately 42.6 hours. It was not heated, and its mass decreased from 11.97 g down to 10.40 g, a 13.1% decrease, which was nearly the same as it was for the heating test.

Even though the mass loss did not show it directly, it is clear from the partial pressure versus time charts, that heating does increase the rate that water is released from the zeolite. It's likely that the majority of the water had already been desorbed from the zeolite by the time it was heated, and even though it was being released faster once it was heated, its mass was insignificant when compared to the overall mass loss that occurred before heating began.

3.3 Dynamic mass change tests

Several preliminary tests were run with samples of NaA type zeolite inside aluminum dishes. The aluminum dishes were set on top of the mass scale while the vacuum chamber was pumped down for several hours. Each sample went into the chamber with close to the same starting mass (~11.95 g), but the amount of water in each of those samples might have been different for each test. The samples are rehyrated by adsorbing water from the open air, but these tests were run before realizing that the amount of time that a sample was given to rehydrate was important, thus not much care was given to keep track of how hydrated a sample was before it went into the vacuum chamber. The samples might have gone into the chamber with the same total mass, but still may have had different amounts of water stored inside them. Figure 3.18 shows how the mass of the samples changed for each of these preliminary test.

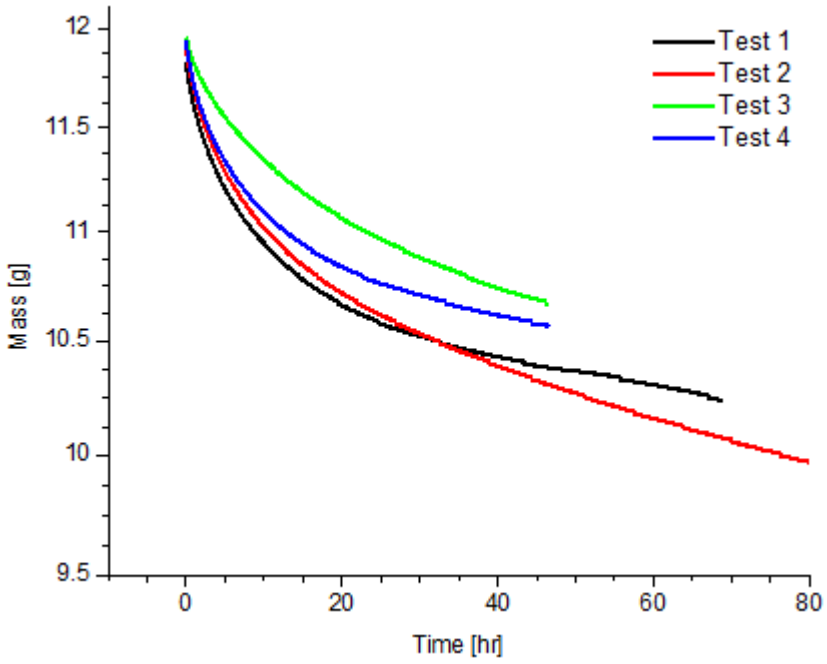

Figure 3.18: Mass of NaA type zeolite versus time in the vacuum chamber during the preliminary dynamic mass change tests.

These plots were fairly consistant, but confirm that samples might not have all been equally saturated before they went into the chamber. To obtain more consistent results,

the next set of tests would use samples that had reached their equilibrium capacity before they went into the chamber. Samples reach equilibrium capacity once they can no longer adsorbing from their environment. To get samples to their equilibrium capacity, they were left in the open air for extended periods of time. Samples would not be used unless their mass had come to a stable position and had not changed significantly ($\Delta m \leq 0.05g$) since the previous day. For most samples, this happened after about 2 days. The next set of tests used larger samples with initial masses in the range of 40-50 grams. Plots of the sample mass versus time in the chamber from theses tests are given in Figure 3.19.

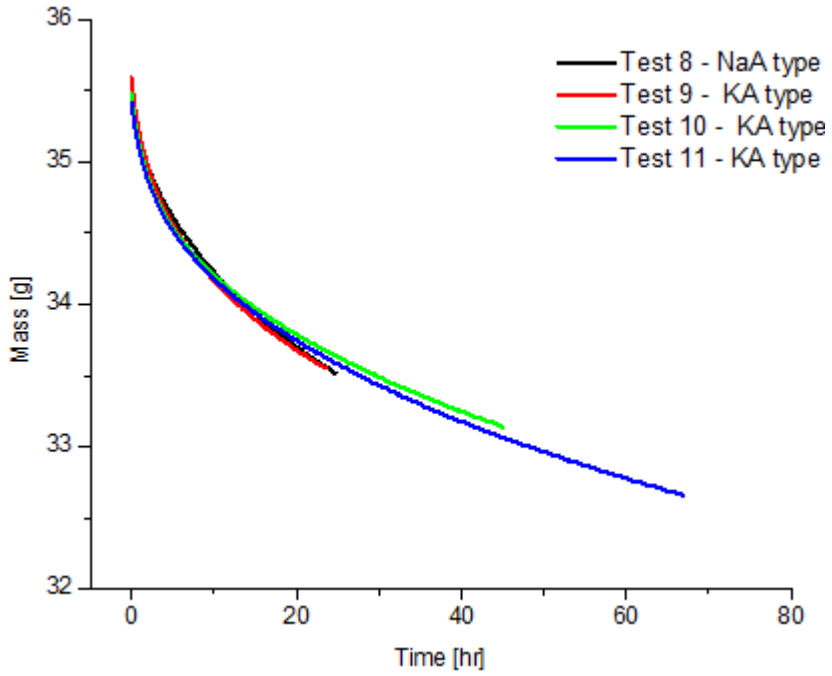

Figure 3.19: Sample mass versus time for the samples that had reached an equilibrium capacity before going into the chamber.

Letting the samples come to full saturation provided much more consistent results than the other tests. These tests also showed that the water would be released at the same rate from the KA type zeolite as it was for the NaA type zeolite. This data was fitted with an exponential curve, given in Figure 3.20, that was used to make predictions on how the mass of a given sample would change during the tests at AEDC.

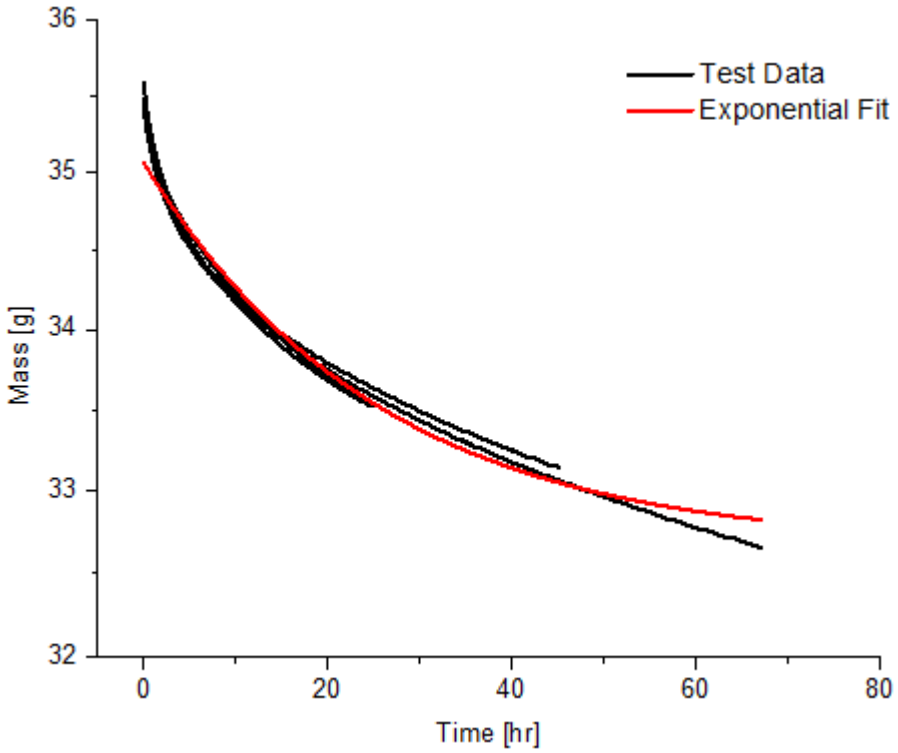

Figure 3.20: Data from dynamic mass change tests 8-11 fitted with an exponential curve.

The equation for the fit is:

$$Mass[g] = (32.66 \pm 0.01) + (2.40 \pm 0.01) \cdot e^{\frac{-time[hr]}{24.7 \pm 0.3}} \tag{3.1}$$

3.4 External chamber tests

Since the zeolite outgased its water without any heating, it was clear that needed to be kept at atmospheric pressure until its water was needed in the experiment. However, keeping the zeolite in an external chamber, and delivering water molecules through a hose to the main vacuum chamber could have a significant impact on the rate at which water is outgassed from the zeolite and how much of that water makes it into the chamber. The external chamber assembly needed to be tested to see how pulling the water vapor through a hose would affect the rate that the water was released from the samples and determine if this method could be used for the tests at AEDC.

3.4.1 Mass loss comparisons

The primary goal of these tests was to see how mass losses of samples inside the external chamber compared to the mass losses recorded with the samples sitting in the middle of the main vacuum chamber. These tests were conducted much like the basic pump down tests were, only samples were put inside the external chamber assembly and not in the main vacuum chamber itself.

As before, dishes were filled with zeolite and left in the open air until they reached an equilibrium capacity. Then 35.85 g samples were measured out and put in glass cylinders inside the external chamber which was valved off from the main chamber. The main chamber was pumped down with the roughing pump for at least five to ten minutes. Then the valve that connected the main chamber to the external chamber was opened to let the roughing pump start pumping down the external chamber. The turbo pump was turned on after the external chamber had already been pumped down by the roughing pump for a while and the pressure in the external chamber had gotten below 500 mTorr.

The amount of time that the samples were left in the chamber varied, but the masses were always recorded as quickly as possible after a sample was removed. There were eight tests in all. The mass that the samples had when they were pulled out of the chamber is plotted against the time they were in the vacuum in Figure 3.21. For comparison, this figure also shows the mass versus time plots from the dynamic mass loss tests.

There was some inconsistency, and as expected, there appears to be a slight decrease in

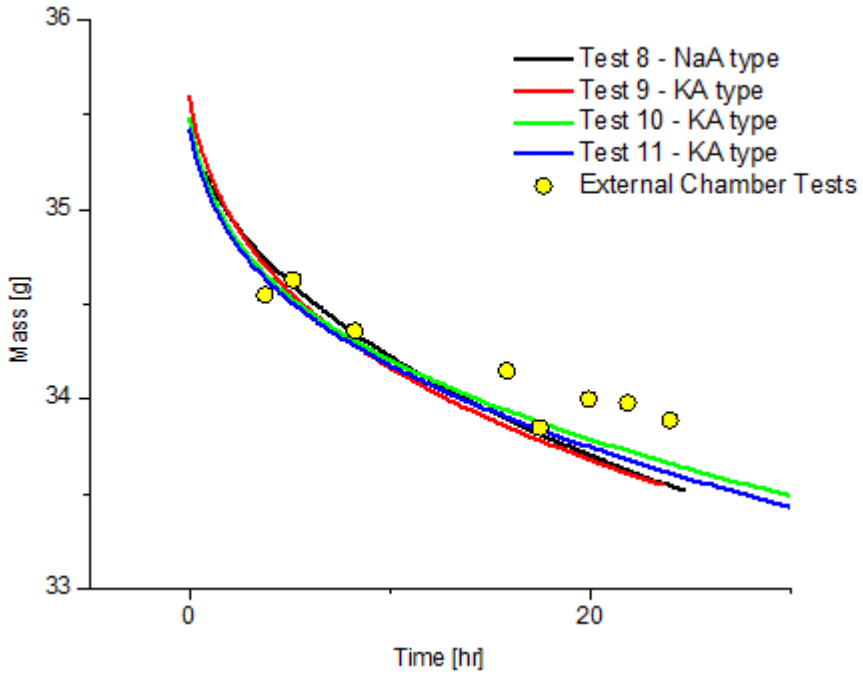

Figure 3.21: Mass versus time for the dynamic mass change and external chamber tests.

the rate at which water was outgassed from the sample in the external chamber. However this did not dramatically reduce the rate at which water was outgassed from the samples.

3.4.2 Residual gas analysis with a sample in the external chamber

The external chamber was also used to get a better idea of what gases were coming from the zeolite. For this test, the vacuum chamber and the external assembly were pumped down for a total of about 5 hours. Then the valve connecting the external chamber assembly to the main chamber was closed to keep any gases coming from the zeolite from going in and being detected by the RGA. The partial pressure of hydrogen, water, nitrogen, oxygen, argon and carbon dioxide were all logged throughout the test and are plotted versus time in Figure 3.22.

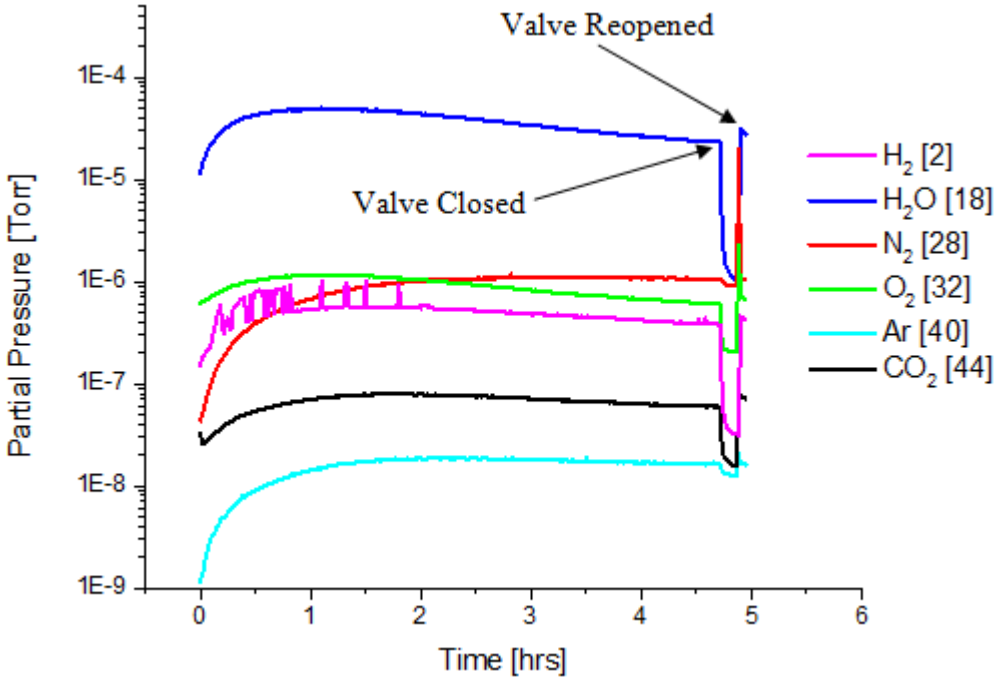

Figure 3.22: Partial pressure of various gases inside the main vacuum chamber throughout the external chamber test.

In addition to this, analog scans were taken before and after the valve to the main chamber was closed. Any gases that appeared in the first scan that did not appear in the second scan were likely to be coming from the zeolite or from leaks somewhere in external chamber assembly. A graph with both analog scans is given in Figure 3.23, and the spectrum analysis for each case is given in Table 3.5.

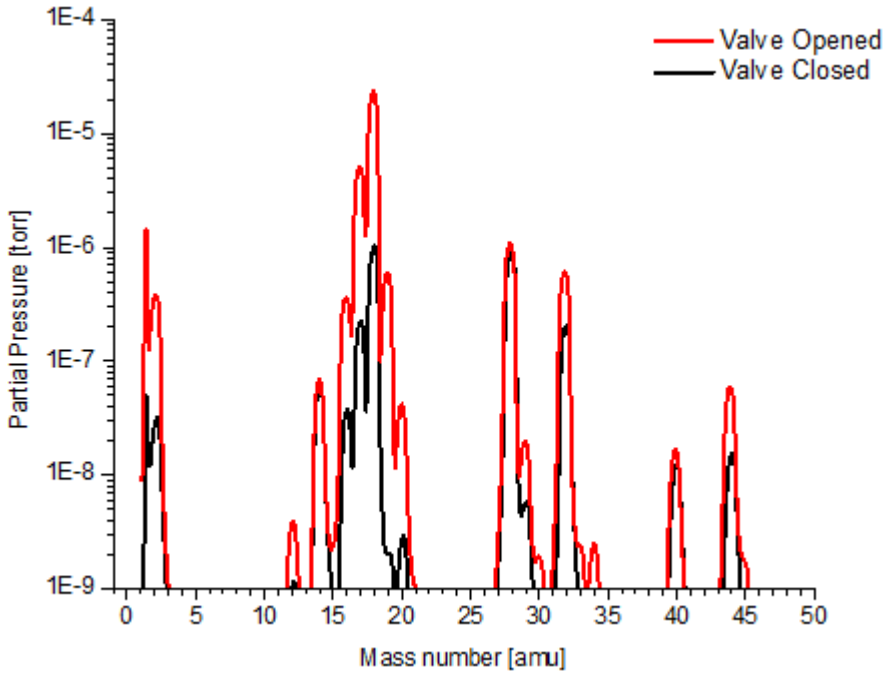

Figure 3.23: Analog scans before and afther the valve connecting the external assembly to the main chamber was closed.

External Chamber	Valve open	Valve closed
Carbon dioxide	0.00%	0.50%
Hydrogen	1.20%	1.20%
Nitrogen	3.50%	34.90%
Oxygen	1.50%	8.00%
Water	93.80%	55.30%

Table 3.5: Spectrum analysis from the external chamber tests.

Subtracting the partial pressures measured after the valve was closed from the partial pressures that were measured while the valve was still opened shows the gases that might be coming from the zeolite and the external chamber with the background gases subtracted. A plots showing the difference between the two analog scans is given in Figure 3.24. The same data is plotted again with a linear vertical scale in Figure 3.25.

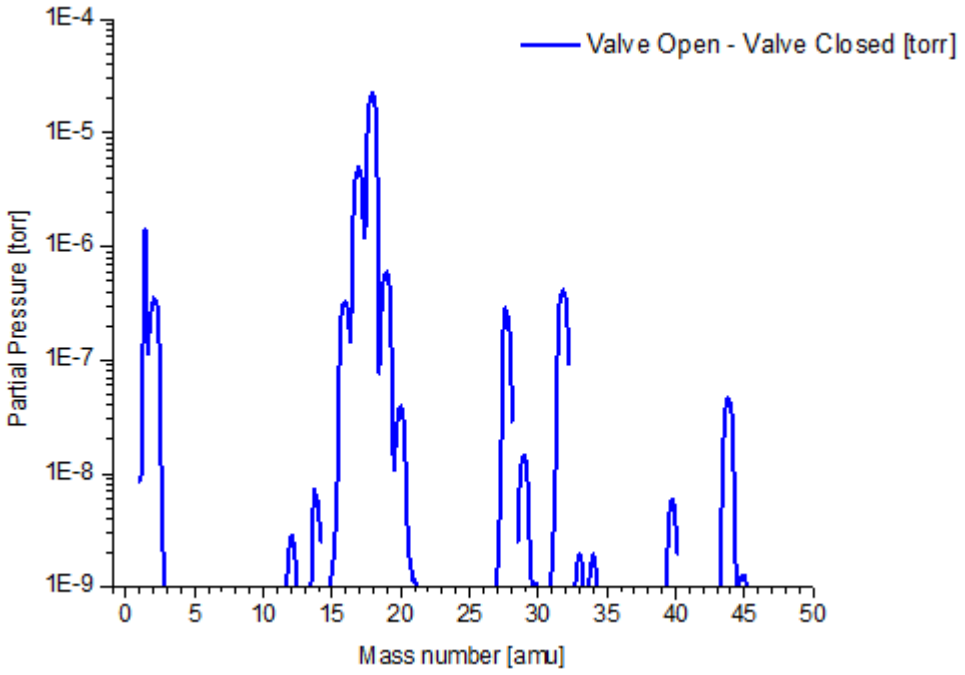

Figure 3.24: Logarithmic plot showing valve open analog scan with the background gases from the valve closed analog scan subtracted.

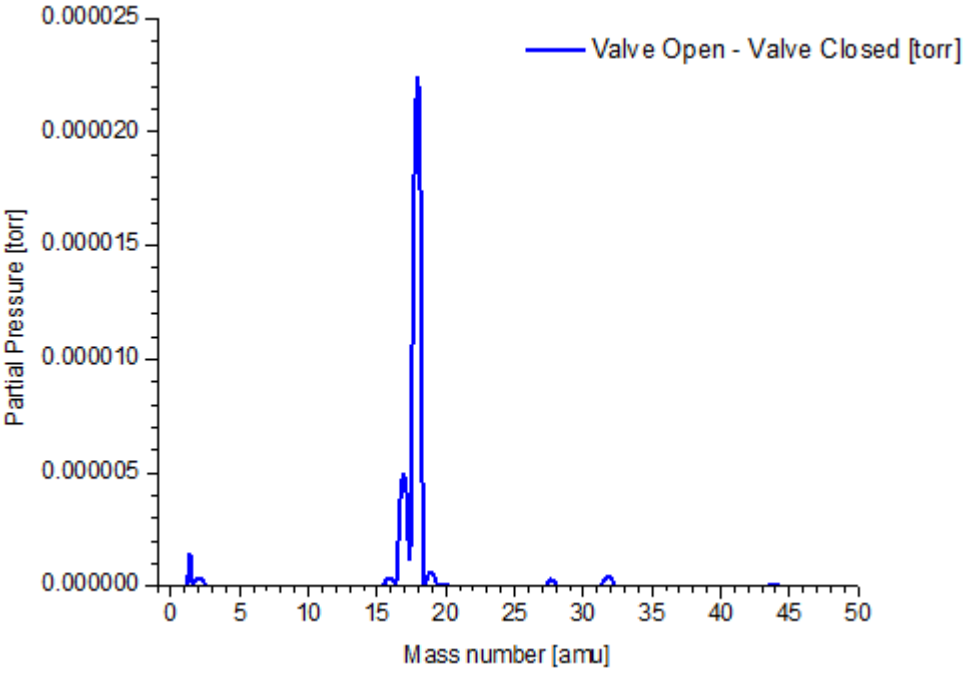

Figure 3.25: Linear plot showing valve open analog scan with the background gases from the valve closed analog scan subtracted.

The difference in the partial pressure of water vapor was $2.15 \cdot 10^{-5}$ torr. The differencese in the partial pressures of H_2, N_2, O_2 and CO_2 were $3.27 \cdot 10^{-7}$, $8.5 \cdot 10^{-8}$, $2.54 \cdot 10^{-7}$ and $3.99 \cdot 10^{-8}$ torr respectively, all of which were nearly two orders of magnitude or more lower than the difference in the partial pressure of water.

3.4.3 Residual gas analysis without a sample in the external chamber

To ensure that none of these gases were coming from leakes in the external chamber assembly, the same residual gas analysis test was done without a sample in the external assembly. After the chamber was pumped down for approximately 22 hrs, the valve connecting the main chamber to the external assembly was closed to see any difference between analog scans taken with the valve open and closed. These analog scans are given in Figure 3.26.

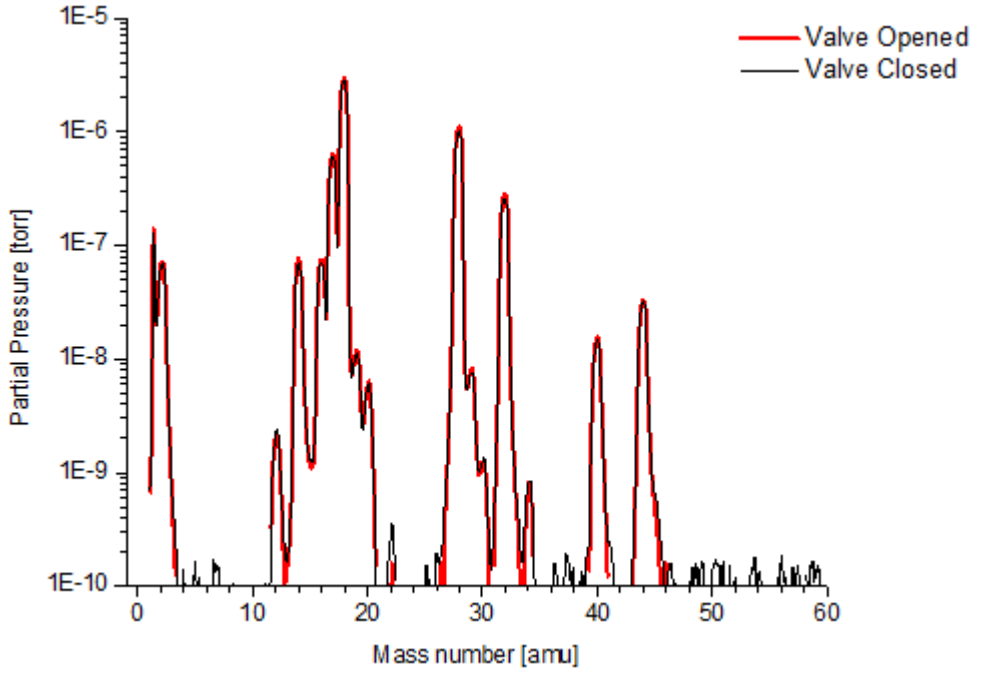

Figure 3.26: Analog scans before and after the valve connecting the external assembly to the main chamber was closed while there was no sample in the chamber.

These scans showed that it was not the external chamber, but the zeolite that was responsible for the major differences in the analog scans taken earlier.

3.4.4 Conclusions about the external chamber assembly

These tests showed that using 3Å zeolite molecular sieves located in an external chamber assembly was a suitable method for introducing water into a vacuum chamber. This method for introducing water vapor to a vacuum chamber was successfully implemented for the second set of cryodeposition tests at AEDC. A few slight modifications were made to the external chamber assembly, and they are described along with and the results from the AEDC tests in the next chapter.

Chapter 4

AEDC tests

4.1 AEDC test setup

A schematic of the modified external chamber assembly as it was used for the cryodeposition tests is given in Figure 4.1. The external chamber was connected to its own pumping system, separate from the main vacuum system. That way, the external chamber assembly could be pumped down quickly to eliminate any unwanted atmospheric gases inside it and reduce the amount of contaminants that would go into the main chamber. This secondary pumping system was attached to the external assembly with a 1/4" I.D. hose that was attached to the leak valve. The thermocouple pressure gauge on the external chamber assembly was replaced with a convectron gauge to obtain more accurate pressure readings at lower pressures.

The external assembly was connected to the main vacuum chamber with a custom feedthrough that was made to convert a 2.75" O.D. Conflat flange on the outside of the chamber into a section of 5/8" O.D. hard copper tubing on the inside of the chamber. The end of that tubing fed into the chamber and connected to a 3" section of 5/8" O.D. stainless steel convoluted tubing. That convoluted tubing was connected to an adapter that connected to a 3/4" schedule 80 aluminum pipe fitting on the back of the effusion cell. The feedthrough and the effusion cell were equipped with heaters to keep them warm and prevent water from freezing inside the line while the chamber was at cryo-temperatures. A similar 1/4" feedthrough was designed for a 10 torr Baratron head and a

type T thermocouple that were used to monitor the pressure and temperature inside the effusion cell.

For the tests at AEDC, the main vacuum chamber and the external assembly were pumped down together until the main chamber reached the conditions needed for cryo-deposition. Then the valve connecting the main chamber and the external assembly was closed and a sample was put inside the external chamber assembly. The secondary pumping system was then turned on to clean out the unwanted atmospheric gases from the external chamber. Once the pressure in the external assembly was sufficiently low ($\sim$100-200 mTorr), the valve to the roughing pump was closed and the valve to the main chamber was re-opened to send the water from the molecular sieves into the main vacuum chamber. If a new sample was needed, the valve to the main chamber was closed, the external chamber was re-opened, and the old sample was replaced with a new one.

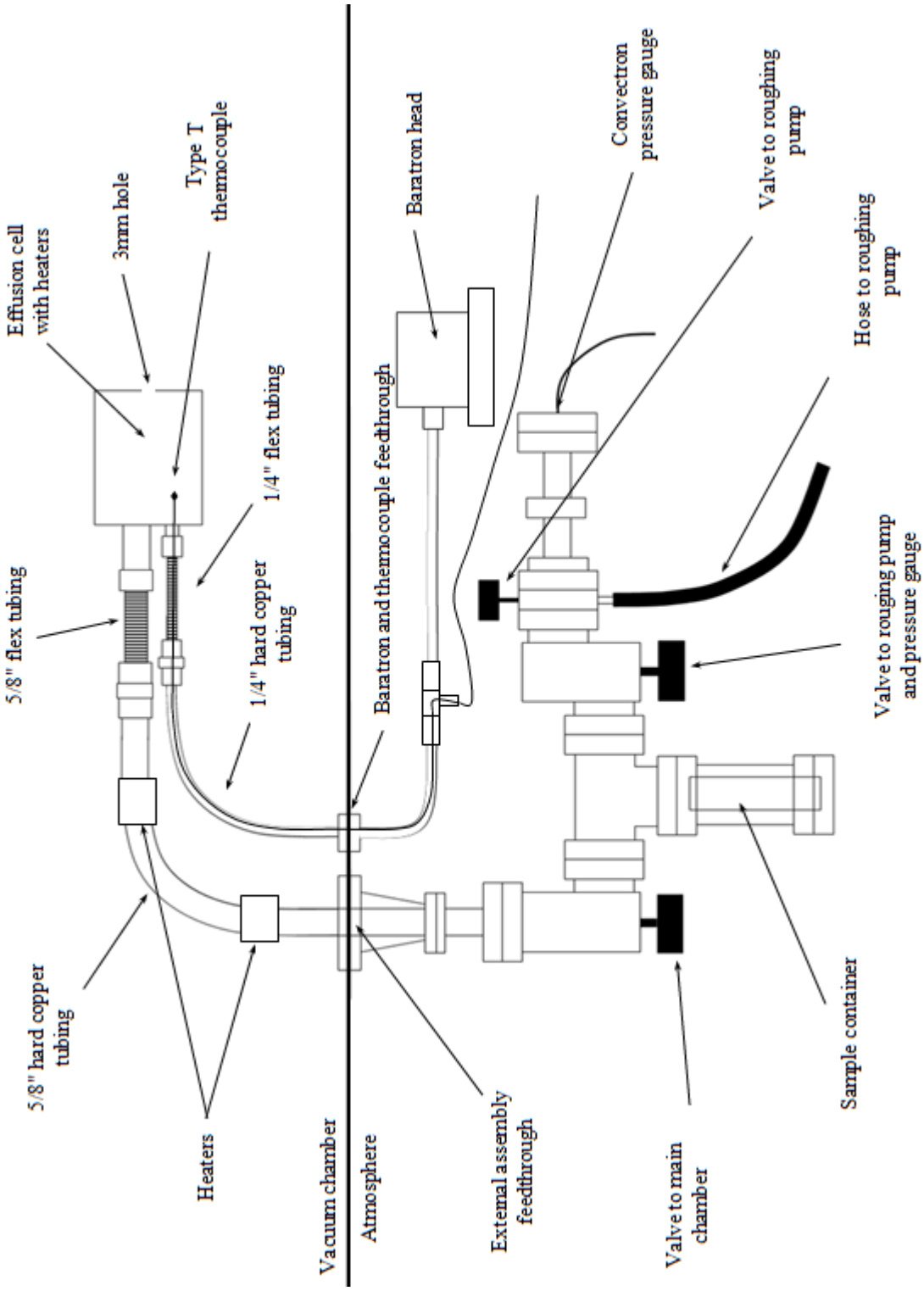

Figure 4.1: External chamber assembly as it was used for the cryodeposition tests at AEDC

4.2 AEDC test results

The tests conducted at AEDC were consistent with the external chamber tests at UTSI. For the first run, a 35.82 g sample was under vacuum for 21 hours and 52 minutes. When the sample was removed from of the external chamber its mass was measured at 33.76 g, a 5.76% decrease. Then, a fresh 35.78 g sample went into the external assembly to replace the old one. This sample was under vacuum for 5 hours and 33 minutes, and when it was taken out of the chamber, its mass was measured at 34.35 g, for a 3.99% mass loss. These results are plotted on a mass versus time chart in Figure 4.2. For comparison, the results from dynamic mass loss tests and external chamber tests are presented there as well.

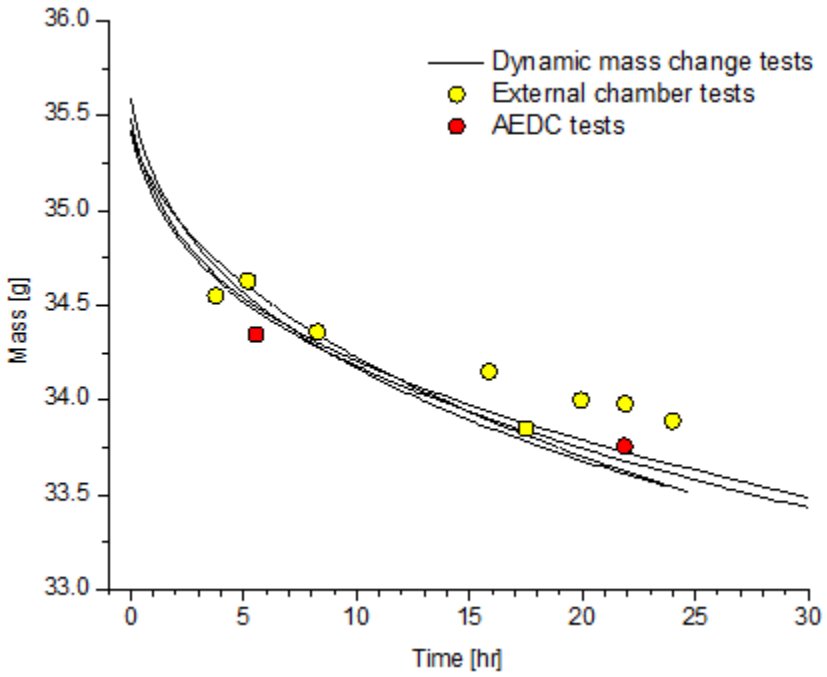

Figure 4.2: Mass versus time chart showing the results from the tests at AEDC.

Chapter 5

Conclusions and Further Work

5.1 Conclusions

The 3Å molecular sieves proved to be the most suitable material for introducing water into the vacuum chamber for the cryodeposition experiments. While the calcium sulfate dihydrate and the cobalt(II) chloride hexahydrate were both capable of releasing water, they were also very fine powders which made them susceptible to being blown around inside the chamber and contaminating the experiment. This potential for failure ultimately made using the calcium sulfate and the cobalt chloride too risky to use.

As a water source, the zeolite behaved just as well, if not better than the other two materials. The Linde 3Å molecular sieves came in a much larger and heavier bead form, which made them much less likely to be blown around inside the chamber than the other two materials were. Like the calcium sulfate and the cobalt chloride, the molecular sieves also held and released nearly pure water. Residual gas analysis did show trace amounts of other gases coming from the zeolite, but the quantities of those gases were relatively insignificant when they were compared to the quantity of water that the zeolite provided. The tests at UTSI showed that the molecular sieves could provide an adsorptive capacity of up to 17.6% without any heating, which is also comparable to the other two materials. Since the molecular sieves released their water without any heating, they needed to be held in their own container, separate from the main vacuum system.

Using this external chamber assembly provided some added flexibility during testing.

Having the ability to change out samples, mid-test, without the need to open up the chamber, allowed tests to be run longer without as much interruption; and having a replenishable water source allowed ice layers to be grown faster and for longer periods of time than was possible before.

After successful tests at AEDC, this study and the described method for introducing water vapor into a vacuum system have been proven beneficial to the ongoing cryodeposition research being conducted at UTSI and AEDC.

5.2 Further Work

A hydrating procedure was developed to saturate the samples with water before they were brought over to AEDC. A schematic of that setup is given in Figure 5.1. This setup was designed to hydrate the molecular sieves in a more humid environment and reduce the amount of unwanted contaminants that they may adsorb. Compressed air was sent through a hose and bubbled in some distilled water. Then the air went through another hose to a flask where it could be directed onto the molecular sieves. Samples that were hydrated with this setup did not have an increased adsorptive capacity, but might have had fewer unwanted contaminates inside them. More test should to be run in order to evaluate the full benefit of this procedure.

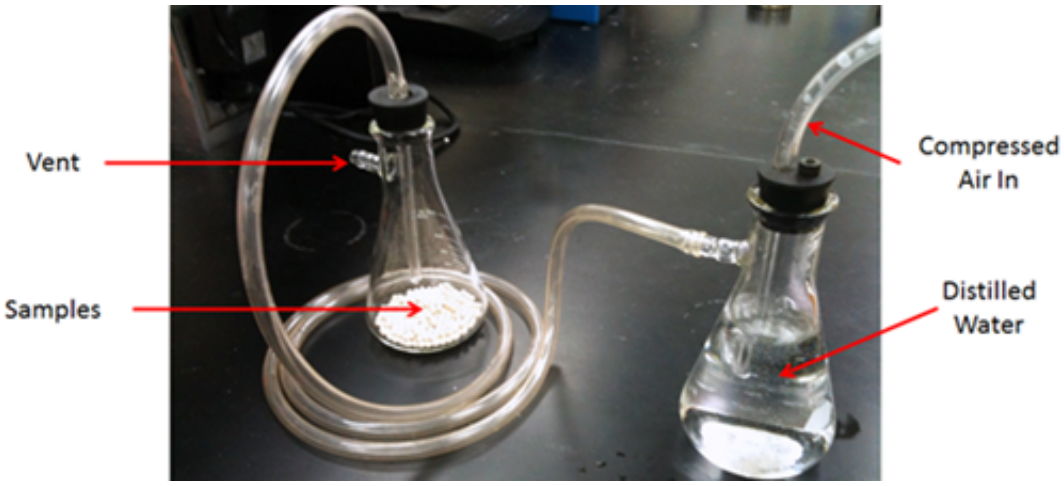

Figure 5.1: Setup for hydrating the molecular sieves.

Tests should be made to see if hydrating the zeolite with this setup had any effect on the zeolites adsorptive capacity and see if this proceedure reduced the amount of unwanted gases adsorbed and later released by the zeolite. Several other steps could also be taken that might help with this as well, and they should be investiaged tool. It is believed that the KA type zeolite adsorbs fewer unwanted gases than the NaA type did; test could be made to confirm if that is the case. The temperature of the zeolite is also supposed to have a significant impact on the size of the pore structures inside it. The diameter of the windows to the α-cage are supposed to 2.9Å at 77 K and 3.3Å at 298 K for the KA type zeolite [4]. Thus, cooling the zeolite during hydration could significantly reduce the amount of unwanted contaminants that the zeolite would adsorb. Heating tests would probably be the best way to compare these different methods, to see what kind of impact they have and to determine how useful they are.

Bibliography

Bibliography

[1] Wikipedia contributors, "Cobalt(II) chloride." http://en.wikipedia.org/w/index.php?title=Cobalt(II)_chloride&oldid=441022817, July 2011.

[2] J. Ribas, A. Escuer, M. Serra, and R. Vicente, "Solid state kinetic parameters of the dehydration of $CoCl_2 \cdot 6H_2O$ by isothermal thermogravimetric measurements," *Thermochimica Acta*, vol. 102, pp. 125–135, 1986.

[3] M. Llano-Restrepo and M. A. Mosquera, "Accurate correlation, thermochemistry, and structural interpretation of equilibrium adsorption isotherms of water vapor in zeolite 3A by means of a generalized statistical thermodynamic adsorption model," *Fluid Phase Equilibria*, vol. 283, pp. 73–88, 2009.

[4] D. W. Breck, *Zeolite Molecular Sieves: Structure, Chemistry, and Use*. John Wiley & Sons, Inc, 1974.

[5] Stanford Research Systems, "Residual Gas Analyzer RGA100, RGA200 and RGA300." http://www.thinksrs.com/products/RGA.htm, 2003.

[6] Wikipedia contributors, "Desiccant." http://en.wikipedia.org/w/index.php?title=Desiccant&oldid=437971221, July 2011.

[7] A. L. Hanson, "Desiccant," in *McGraw Hill Encyclopedia of Science and Technology*, McGraw Hill, 9th ed., 2002.

[8] "Desiccant," in *Dictionary of Engineering Materials*, John Wiley & Sons Inc., 2004.

[9] Wikipedia contributors, "Sorption." http://en.wikipedia.org/w/index.php?title=Sorption&oldid=433355205, June 2011.

[10] "Adsorption," in *Encyclopedia Britanica*, Encyclopedia Britannica Inc., 15th ed., 2002.

[11] H. Liebeskind, "Absorption," in *Encyclopedia Americana*, Grolier Inc., international ed., 1998.

[12] H. Liebeskind, "Adsorption," in *Encyclopedia Americana*, Grolier Inc., international ed., 1998.

[13] Sorbent Systems, "Desiccants: Technical Data and Terminology." `http://www.sorbentsystems.com/desiccants_terminology.html#adsorption`, 2006.

[14] *Handbook of Chemistry & Physics 91st Edition*. CRC Press, Taylor and Francis Group, LLC, 2011.

[15] H. Liebeskind, "Calcium sulfate," in *Encyclopedia Americana*, Grolier Inc., international ed., 1998.

[16] Wikipedia contributors, "Calcium sulfate." `http://en.wikipedia.org/w/index.php?title=Calcium_sulfate&oldid=442140244`, July 2011.

[17] B. Molony and M. J. Ridge, "Kinetics of the dehydration of calcium sulfate dihydrate in vacuo*," *Australian Journal of Chemistry*, vol. 21, pp. 1063–1065, 1968.

[18] P. S. R. Prasad, "In situ micro-raman investigation of dehydration mechanism in natural gypsum," *Current Science*, vol. 80, no. 9, pp. 1203–1207, 2001.

[19] K. M. Robertson and D. L. Bish, "Therman behavior of the calcium-sulfate-h_2o system," in *40th Lunar and Planetary Science Conference*, 2009.

[20] J. J. Gardet, "The dehydration kinetics of calcium sulphate dihydrate influence of the gaseous atmosphere and the temperature," *Cement and Concrete Research*, vol. 6, pp. 697–706, 1976.

[21] C. A. Strydom, D. L. Hudson-Lamb, J. H. Potgieter, and E. Dagg, "The thermal dehydration of synthetic gypsum," *Thermochimica Acta*, vol. 269/270, pp. 631–638, 1995.

[22] "Cobaltous chloride" and "cobaltous chloride hexahydrate," in *Dictionary of Engineering Materials*, John Wiley & Sons Inc., 2004.

[23] VWR, "Cobalt(II) chloride MSDS." `https://www.vwrsp.com/msds/10/AA1/AA10692-09.pdf`, May 2010.

[24] "Zeolite," in *Encyclopedia Britanica*, Encyclopedia Britannica Inc., 2002.

[25] "Molecular sieve," in *Encyclopedia Britanica*, Encyclopedia Britannica Inc., 15th ed., 2002.

[26] Grace Davison, "Zeolite Molecular Sieve." `http://lartpc-docdb.fnal.gov/0000/000084/001/zeolite_molecular_sieve.pdf`, Febuary 2006.

[27] Sorbent Systems, "Desiccant Types." `http://www.sorbentsystems.com/desiccants_types.html#mole`, 2006.

[28] Wikipedia contributors, "Molecular sieve." `http://en.wikipedia.org/w/index.php?title=Molecular_sieve&oldid=440175977`, July 2011.

[29] D. W. Breck, "Crystalline molecular sieves," *Journal of Chemical Education*, vol. 41, pp. 678–689, December 1964.

[30] "Zeolite," in *Van Nostrand's Scientific Encyclopedia*, John Wiley & Sons Inc., 9th ed., 2002.

[31] A. Dyer, *An Introduction to Zeolite Molecular Sieves*. John Wiley & Sons, Inc, 1988.

[32] Desiccantpacks.net, "Molecular sieve." `http://www.desiccantpacks.net/molecular-sieve/`, 2011.

[33] R. T. Yang, *Adsorbents: Fundamentals and Applications*. John Wiley & Sons, Inc, 2003.

[34] C. D. Chudasama, J. Sebastian, and R. V. Jasra, "Pore-size engineering of zeolite A for the size/shape selective molecular separation," *Ind. Eng. Chem. Res.*, vol. 44, pp. 1780–1786, 2005.

[35] R. D. Shannon, "Revised effective ionic radii and systematic studies of interatomic distances in halides and chalcogenides," *Acta Crystallographica Section A*, vol. 32, pp. 751–767, Sep 1976.

[36] W. J. Moore, *Physical Chemistry 3rd Ed.* Prentice-Hall Inc., 1962.

[37] Stanford Research Systems, *Operating Manual and Programming Reference: Models RGA 100, RGA200, and RGA300 Residual Gas Analyzer*, 1996.

[38] Wikipedia contributors, "Atmosphere of earth." `http://en.wikipedia.org/w/index.php?title=Atmosphere_of_Earth&oldid=443112891`, August 2011.

[39] D. H. Herring, "Leak rates, leak detection and leak repair," *Industiral Heating*, July 2010.

[40] R. Honig, "Vapor pressure data for the solid and liquid elements," *RCA Review*, vol. 23, pp. 567–586, 1962.

Vita

James Philip Rogers was born and raised in Columbia Tennessee. He was awarded a Bachelor's of Science degree in physics from Tennessee Technological University in Cookeville, Tennessee. He sought further studies at the University of Tennessee Space Institute in Tullahoma, where he is currently being awarded his Master's of Science degree in aerospace engineering. James intends to pursue a doctorate degree to further his education in physics and engineering. His professional interests center around space technology.